Radiative quark mass and mixing hierarchies from supersymmetric models with a fourth mirror family

Alexander L. Kagan
Department of Physics and Astronomy, University of Maryland at College Park, College Park, Maryland 20742
(Received 6 February 1989)

A class of supersymmetric models is discussed in which radiative quark mass as well as Kobayashi-Maskawa (KM) and neutral-current mixing hierarchies are obtained with all Yukawa couplings of the same order and no horizontal symmetries. The presence of a single mirror family is crucial. The respective KM mixing angles of the top quark and mirror top quark (t') are of the same order (in particular, $V_{tb} \sim V_{t'b} \sim 1$). The lighter of the two top quarks typically has a mass $\lesssim 100$ GeV while the mirror bottom quark, considerably heavier than either top quark, typically has a mass $\lesssim 300$ GeV. The main experimental consequence of the neutral-current mixing matrix is $B(Z \to \bar{c}t + c\bar{t}) \sim 10^{-4} - 10^{-5}$ (if $m_t < m_Z - m_c$), with similar branching ratio for charm + mirror top quark. These decays should be observable at CERN LEP given 10^7 Z's. The models provide a promising framework for nonperturbative Maiani-Parisi-Petronzio unification. The field content can, in principle, be obtained from the superstring and a search for two-generation string vacua is advocated.

I. INTRODUCTION

In both the up- and down-quark sectors there exists a mass hierarchy[1] with $m_u/m_c \sim \frac{1}{200}$, $m_c/m_t \lesssim \frac{1}{40}$, $m_d/m_s \sim \frac{1}{20}$, and $m_s/m_b \sim \frac{1}{30}$. There is also a Kobayashi-Maskawa (KM) mixing angle hierarchy with $V_{us} \sim 0.22$, $V_{cb} \sim 0.05$, and $V_{ub} \sim V_{us} V_{cb}$. The quark isodoublet mass splittings satisfy $m_t \gg m_b$, $m_c \gg m_s$, and $m_d > m_u$. In the standard model there is no understanding of these hierarchies as they are put in by hand at the tree level via a Yukawa coupling hierarchy of order 10^4. Many authors[2] have proposed that the masses of the first and second generations may arise out of radiative corrections whereas those of the third generation may be present at the tree level, thereby reducing reliance on Yukawa coupling hierarchies. In the context of such proposals it would be natural to expect that quark mixing as well as isodoublet mass splittings could also be understood in terms of radiative corrections.

Recently, a radiative mechanism has been discussed in Refs. 3 and 4 for obtaining quark mass and mixing hierarchies without the need for a Yukawa coupling hierarchy (they can all be ~ 1). In contrast with previous attempts along this direction, this approach does not require the existence of a horizontal symmetry distinguishing among the three known families. The third-generation quarks acquire mass at the tree level while the second- and first-generation quarks acquire their mass at one and two loops, respectively. The basic ingredients are as follows.

(i) The addition of a single exotic family of quarks Q, Q^c with large tree-level masses, M_U, M_D, whose quantum numbers differ from those of the ordinary quarks q_i, q_i^c, $i = 1,2,3$. The exotic family mixes with the latter at the tree level via mass terms

$$a_L h_{Li} q_i Q^c + q_R h_{Ri} q_i^c Q \ ,$$

where $a_{L,R}$ are massive parameters and $h_{L,R}$ are dimensionless coupling vectors, normalized to unity.

(ii) An isosinglet, charged color-triplet scalar ω with Majorana-type rank-three couplings to ordinary quarks[5] of the form

$$H_{ij}^L \omega q_i q_j + H_{ij}^R \omega q_i^c q_j^c \ .$$

From (i) the tree-level mass matrix is of the form

$$\begin{array}{c} \\ q_i \\ Q \end{array} \begin{array}{c} \begin{array}{cc} q_i^c & \qquad Q^c \end{array} \\ \begin{pmatrix} 0 & \cdots & a_L |h_L\rangle \\ \vdots & & \vdots \\ a_R \langle h_R | & \cdots & M \end{pmatrix} \end{array} ,$$

inducing a mass contribution for ordinary quarks of the form

$$m^{(0)} |h_L\rangle \langle h_R| \ .$$

Only one ordinary quark family acquires mass at the tree level[6] ($= m^{(0)}$) because this contribution is of unit rank. In the seesaw limit $M \gg a_L, a_R$, $m^{(0)}$ is given by $-a_L a_R / M$. From (ii) a radiative structure emerges, see Figs. 1(a) and 1(b), again leading to rank-one mass contributions of the form

$$m^{(1)} H^L |h_L\rangle \langle h_R| H^R + m^{(2)} H^{L2} |h_L\rangle \langle h_R| H^{R2} \ .$$

Because radiative contributions are also of unit rank only one additional quark family picks up mass at each loop order[3] and a mass hierarchy emerges for the ordinary quarks.

A purely radiative KM mixing hierarchy obtains[4] if

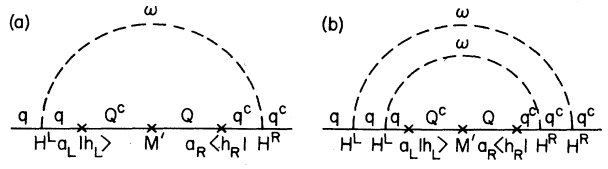

FIG. 1. Diagram (a) is a unit-rank one loop graph contributing to second-generation masses and diagram (b) is a unit-rank two-loop graph contributing to first-generation masses.

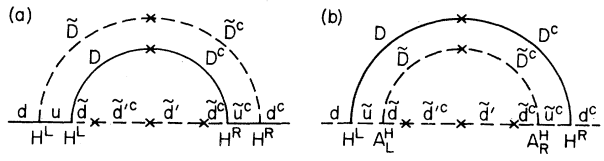

FIG. 3. Two-loop graphs contributing to $\delta M_{(2)}$.

$|h_L\rangle^u = |h_L\rangle^d$ since in this case the left-handed up and down tree-level mass eigenstates are aligned in the three-generation subspace spanned by q_i, $i=1,2,3$. Subsequent rotation between the two sets of mass eigenstates in this subspace results from radiative corrections. The observed quark isodoublet mass splittings obtain[4] if $M_D \gg M_U$. For the third family this is clear from the seesaw expression for $m^{(0)}$. For the first and second families the fact that ω is charged is crucial for this result since the one-loop graph [Fig. 1(a)] contributing to up-(down-) quark masses contains the mass insertion M_D (M_U) while for the two-loop graph [Fig. 1(b)] the situation is reversed. Radiative flavor-changing Z couplings, satisfying

$$Zq_2q_3 \gg Zq_1q_3 \gg Zq_1q_2 ,$$

emerge as well, cf. Sec. VI (Ref. 7).

The exotic family of quarks in Refs. 3 and 4 consists of isosinglet up and down vectorlike quarks with masses in the TeV range. Here we consider an alternative supersymmetric implementation of the radiative mechanism in which the exotic up and down quarks belong to a single mirror family.[8] As it turns out, the graphs of Fig. 1 provide negligible mass contributions in this case (cf. Sec. III B) and, instead, the dominant one- and two-loop graphs (Figs. 2 and 3, respectively) contain the fermionic superpartner of the color-triplet scalar as well as squarks in the loops. Hence supersymmetry is crucial for success of these models. Gluino graphs (Fig. 4) can also be important for the light-quark mass spectrum.

The choice of a mirror family has several interesting consequences which we enumerate below.

(1) Equality of $|h_L\rangle^{u,d}$, required to obtain a radiative KM hierarchy, follows directly from $SU(2)_L$ invariance.

(2) The inequality $M_D \gg M_U$, required for obtaining the observed quark isodoublet mass splittings, is associated with the $SU(2)_L$-breaking vacuum alignment and can be obtained without explicit isospin breaking in the superpotential. Supersymmetry plays an important role here as well.

(3) ρ parameter constraints on isodoublet mass splitting[9] imply that the lighter of the two top quarks (ordinary and mirror) will, for reasonable choices of parameters, have a mass $\lesssim 100$ GeV, while the mirror bottom quark, considerably heavier than either top quark, will have a mass $\lesssim 300$ GeV. Because V_{tb}, $V_{t'b} \sim 1$, where t and t' are the top and mirror top quarks, respectively, these models have potentially rich implications for top-quark searches at hadronic colliders.

(4) The $Zct^{(\prime)}$ coupling will be large, $\sim 10^{-2}$, implying $B(Z \to c\bar{t}^{(\prime)} + \bar{c}t^{(\prime)}) \sim 10^{-4}-10^{-5}$ if $m_{t^{(\prime)}} < m_Z - m_c$. These decays should be observable at CERN LEP, assuming 10^7 Z's. The $Z\,db$ coupling may be large enough to induce B_d-$\bar{B}_d$ mixing at the observed[10] level via tree-level Z exchange. Finally, reductions in forward-backward asymmetry from standard-model expectations for $e^+e^- \to b\bar{b}$, $t\bar{t}$ can be as large as 10%, 30–100 %, respectively, due to mixing of ordinary and mirror quarks.

(5) Because of supersymmetry the field content of these models provides a very promising framework for nonperturbative Maiani-Parisi-Petronzio (MPP) unification.[11,12] It follows that observed low-energy gauge couplings may be obtained from initial couplings of order unity. If this is indeed the case then *all dimensionless couplings, Yukawa as well as gauge, could be ~ 1 at M_P.*

(6) The field content required is standard from an SO(10) or E_6 point of view, with all matter and Higgs fields (not including gauge singlets) obtainable from **16**'s, $\overline{\mathbf{16}}$'s, **10**'s of SO(10), or **27**'s, $\overline{\mathbf{27}}$'s of E_6. Therefore this class of models is, in principle, obtainable from the superstring. Because there are three ordinary and one mirror families one must search for two-generation vacua.

The organization of the paper is as follows. In Sec. II the field content, interactions, and vacuum alignment are presented for this class of models. Detailed discussion of the tree-level and radiative mass structure follows in Sec. III. Results of a perturbative calculation of quark masses and eigenstates are given in Sec. IV. The KM and neutral-current mixing matrices are studied in Secs. V and VI, respectively, the latter including discussion of

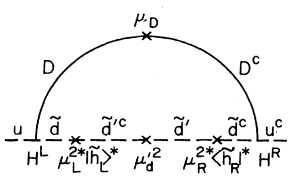

FIG. 2. Squark-isosinglet quark graph contributing to δM_D.

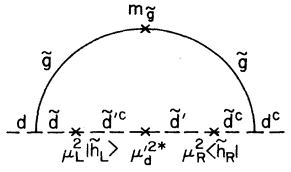

FIG. 4. Squark-gluino graph contributing to $\delta M_{\tilde{g}}$.

phenomenological consequences. In Sec. VII we remark on nonperturbative MPP unification within the context of this class of models and in Sec. VIII we conclude with a summary of our results.

II. THE SUPERSYMMETRIC MIRROR MODELS

A. The field content and interactions

The class of models to be discussed is supersymmetric, with soft supersymmetry breaking assumed, and requires three ordinary generations and one mirror generation. Supersymmetry is crucial for many of the models' successes. The electroweak gauge groups ($G_{\rm EW}$) included in the discussion are $SU(2)_L\otimes SU(2)_R\otimes U(1)_{B-L}$ (G_{LR}), $SU(2)_L\otimes U(1)_R\otimes U(1)_{B-L}$ (G_{1R}), and $SU(2)_L\otimes U(1)_Y$ (G_{1Y}). For reasons of economy the field content as well as the Lagrangian will be presented in left-right-symmetric notation.

The full symmetry group is

$$G=SU(3)_c\otimes G_{\rm EW}\otimes Z_3\otimes Z_2 \ . \tag{2.1}$$

The role of the discrete group will be clarified later in this section. For G_{LR} the superfield content of the matter and Higgs sectors together with transformation properties under G are given in Tables I and II, respectively. Tildes indicate scalars. The mirror family, denoted by Q'^c, Q', is primed and charge conjugated with respect to the ordinary families. The isosinglet down-quark superfields D, D^c together play the role of ω (see Figs. 1–3). For G_{1R} and G_{1Y} the matter sector remains the same, with the appropriate gauge quantum numbers understood, while in the Higgs sector the charged components e^c, e' of the would-be $SU(2)_R$ Higgs doublets are omitted.

For G_{LR} the most general superpotential W, consistent with the transformation properties of Tables I and II, is

$$W=W_M+W_H \ , \tag{2.2}$$

with the matter-Higgs superpotential W_M given by

$$\begin{aligned}W_M=&H_{ij}^L Q_{Li}Q_{Lj}D+H_{ij}^R Q_{Ri}^c Q_{Rj}^c D^c+\lambda_1 Q_L'^c\phi Q_R'\\&+h_{Li}\rho Q_{Li}Q_L'^c+h_{Ri}\rho Q_{Ri}^c Q_R'+\mu_D DD^c\end{aligned} \tag{2.3}$$

and the purely Higgs superpotential W_H given by

$$\begin{aligned}W_H=&\lambda_2 H_L'^c\phi H_R'+\lambda_L\rho H_L H_L'^c+\lambda_R\rho H_R^c H_R'+\lambda_3\rho^3\\&+\lambda_4 y\phi^2+\lambda_5 y^3+\mu\rho y \ .\end{aligned} \tag{2.4}$$

The quantities H_{ij}^L, H_{ij}^R, λ_i, h_{Li}, h_{Ri} are dimensionless couplings and are taken to be ~ 1. The massive parameters μ, μ_D are $\sim 1-10$ TeV and, of course, can be replaced by couplings of a gauge singlet, neutral with respect to $Z_3\otimes Z_2$, which acquires a comparable vacuum expectation value (VEV). The couplings of ρ lead to ordinary-mirror mixing while those of y (Ref. 13) ensure that all charged components of ϕ will be massive. For future reference some of the Yukawa couplings of interest are written below in terms of components (generation indices are dropped):

$$\begin{aligned}&Q_L'^c\phi Q_R'=u'^c u'\tilde N_E+d'^c d'\tilde\nu_E+d'^c u'\tilde E_N+u'^c d'\tilde E_\nu+\cdots \ ,\\&Q_L Q_L D=ud\tilde D+\cdots \ ,\\&H_L'^c\phi H_R'=e'^c e'\tilde\nu_E+\nu'^c N'\tilde N_E-e'^c N'\tilde E_N-\nu'^c e'\tilde E_\nu+\cdots \ .\end{aligned} \tag{2.5}$$

The soft supersymmetry-breaking scalar potential is given by

TABLE I. Quark superfield content in left-right-symmetric notation.

LH matter superfields	$G=3\times 2_L\times 2_R\times 1_{B-L}\times Z_3\times Z_2$	LH fermionic components
$Q_{i=1,2,3}$	$(3,2,1,\frac{1}{3},0,0)$	$Q=\begin{bmatrix}u\\d\end{bmatrix}$
$Q_{i=1,2,3}^c$	$(\bar 3,1,2,-\frac{1}{3},0,0)$	$Q^c=\begin{bmatrix}u^c\\d^c\end{bmatrix}$
Q'^c	$\left(\bar 3,2,1,-\frac{1}{3},\frac{2\pi}{3},0\right)$	$Q'^c=\begin{bmatrix}u'^c\\d'^c\end{bmatrix}$
Q'	$\left(3,1,2,\frac{1}{3},\frac{2\pi}{3},0\right)$	$Q'=\begin{bmatrix}u'\\d'\end{bmatrix}$
D	$(3,1,1,-\frac{2}{3},0,0)$	D
D^c	$(\bar 3,1,1+\frac{2}{3},0,0)$	D^c

$$V_{\text{soft}} = A^H_{Lij}\tilde{Q}_{Li}\tilde{Q}_{Lj}\tilde{D} + A^H_{Rij}\tilde{Q}^{\,c}_{Ri}\tilde{Q}^{\,c}_{Rj}\tilde{D}^{\,c} + A_1\tilde{Q}'^{c}_{L}\tilde{\phi}\tilde{Q}'_{R} + A^Q_{Li}\tilde{\rho}\tilde{Q}_{Li}\tilde{Q}'^{c}_{L} + A^Q_{Ri}\tilde{\rho}\tilde{Q}^{\,c}_{Ri}\tilde{Q}'_{R} + A_2\tilde{H}'^{c}_{L}\tilde{\phi}H'_R + A_L\tilde{\rho}\tilde{H}_L\tilde{H}'^{c}_{L}$$
$$+ A_R\tilde{\rho}\tilde{H}^{\,c}_{R}\tilde{H}'_R + A_3\tilde{y}\tilde{\phi}^2 + A_4\mu_D\tilde{D}\tilde{D}^{\,c} + A_5\tilde{\rho}^3 + A_6\tilde{y}^3 + A_7\mu\tilde{\rho}\tilde{y} + \text{H.c.} + \sum m^2_{\tilde{\phi}_i}|\tilde{\phi}_i|^2 + \sum m_{\tilde{g}_i}\tilde{g}^2_i\,, \tag{2.6}$$

where the summation is over all scalar fields and gauginos, respectively. The mass parameters A, m_{ϕ_i}, $m_{\tilde{g}_i}$ are taken to be $\lesssim m_{\text{SUSY}}$, where m_{SUSY}, the scale of soft supersymmetry breaking, is chosen to be $\sim 1-10$ TeV. For G_{1R} the most general superpotential W and scalar potential V_{soft} are the same as above with terms involving e^c, e' omitted and appropriate couplings understood in (2.3)–(2.6). For G_{1Y} there will be additional terms involving N^c, N' in W_H, and involving their scalar components in V_{soft} attributed to the fact that these fields are gauge singlets in this case. However these terms do not alter the physics significantly as far as we are concerned and we do not include them here. In addition to V_{soft} there will be F^2 terms in the scalar potential given by $\sum|\partial W(\tilde{\phi})/\partial\tilde{\phi}|^2$, where the sum is over all scalar fields and $W(\tilde{\phi})$ denotes W with superfields replaced by their scalar components. There will also be quartic D^2 terms associated with the gauge interactions. Specific terms in the F^2 and D^2 sectors of the scalar potential will be given when necessary.

The desired Higgs VEV pattern is given by

$$\langle N'\rangle, \langle N^c\rangle \sim 10^3 - 10^4 \text{ GeV}, \ \langle \nu_E\rangle \sim \Lambda_F\,,$$
$$\langle \nu_E\rangle \gg \langle N_E\rangle, \langle \nu'^c\rangle, \langle \nu\rangle\,, \tag{2.7}$$
$$\langle \rho\rangle, \langle y\rangle \sim 10^2 - 10^3 \text{ GeV}\,.$$

$\text{SU}(2)_L$ is broken primarily via $\langle \nu_E\rangle$. A light neutrino solution may require additional Higgs fields with large intermediate-mass scale VEV's. For example, for G_{LR} a Majorana seesaw may require an $\text{SU}(2)_R$ Higgs doublet with a VEV $\gtrsim 10^{10}-10^{11}$ GeV. Therefore $\text{SU}(2)_R$ or $\text{U}(1)_R$ as well as the discrete group may be broken at scales considerably larger than $\langle N'\rangle$, $\langle N^c\rangle$. The problem of neutrino masses will be discussed in detail elsewhere.

B. Remarks on the vacuum alignment

The discrete symmetry does not distinguish between the ordinary generations hence it is not a horizontal symmetry. Rather, it distinguishes between ordinary and mirror matter, the latter transforming differently with respect to the gauge interactions. Its role is to ensure that ordinary quarks do not couple to ϕ, H_L, H^c_R, H'^c_L, H'_R at the tree level. As a result the first two generations are massless at the tree level. $\langle\tilde{\rho}\rangle$ and $\langle\tilde{\phi}\rangle$ lead to tree-level masses for the third and mirror families. The choice of $Z_3\otimes Z_2$ is not unique. For example, a Z_4 symmetry can accomplish the same result.

For left-right-symmetric models (which are isospin invariant) the observed intragenerational quark mass hierarchies must result from spontaneous isospin breaking. In Sec. III we show that the crucial relation is $\langle \nu_E\rangle \gg \langle N_E\rangle$, as in (2.7). Even for non-left-right-symmetric models the inequality is desirable since it

TABLE II. Higgs superfield content in left-right-symmetric notation.

LH Higgs superfields	$G = 3\times 2_L\times 2_R\times 1_{B-L}\times Z_3\times Z_2$	Scalar components
ϕ	$\left[1,2,2,0,\frac{2\pi}{3},0\right]$	$\tilde{\phi} = \begin{bmatrix}\tilde{N}_E & \tilde{E}_\nu\\ \tilde{E}_N & \tilde{\nu}_E\end{bmatrix}$
H_L	$(1,2,1,-1,0,\pi)$	$\tilde{H}_L = \begin{bmatrix}\tilde{\nu}\\ \tilde{e}\end{bmatrix}$
H^c_R	$(1,1,2,1,0,\pi)$	$\tilde{H}^{\,c}_R = \begin{bmatrix}\tilde{N}^{\,c}\\ \tilde{e}^{\,c}\end{bmatrix}$
H'^c_L	$\left[1,2,1,1,\frac{2\pi}{3},\pi\right]$	$\tilde{H}'^{c}_{L} = \begin{bmatrix}\tilde{\nu}'^{c}\\ \tilde{e}'^{c}\end{bmatrix}$
H'_R	$\left[1,1,2,-1,\frac{2\pi}{3},\pi\right]$	$\tilde{H}'_R = \begin{bmatrix}\tilde{N}'\\ \tilde{e}'\end{bmatrix}$
ρ	$\left[1,1,1,0,-\frac{2\pi}{3},0\right]$	$\tilde{\rho}$
y	$\left[1,1,1,0,+\frac{2\pi}{3},0\right]$	$\tilde{y}$

reduces the degree of explicit isospin breaking required in the Yukawa sector. This inequality follows naturally from the presence of the VEV $\langle N' \rangle$ [see (2.7)], without the need for explicit isospin breaking in the superpotential.[14] Briefly, this is because via F^2 terms the scalars $\tilde{N}_E$, $\tilde{\nu}$ acquire additional large positive-mass contributions $\sim\lambda_2^2\langle N' \rangle^2$ which $\tilde{\nu}_E$ does not since there is no trilinear in the Higgs superpotential coupling ν_E and N' [see (2.4) and (2.5)]. As a result, $m^2_{\tilde{N}_E}, m^2_{\tilde{\nu}^c}$ can be large and positive while $m^2_{\tilde{\nu}_E}$ can remain small or negative, leading to the desired hierarchy. Supersymmetry is crucial for this result since global symmetries cannot ensure the absence of the gauge-invariant terms $|\tilde{\nu}^c_E|^2|\tilde{N}'|^2$, $|\tilde{\nu}^c_E|^2|\tilde{N}^c|^2$ from the scalar potential of a nonsupersymmetric model. On the other hand, in supersymmetric models the scalar potential, including quartic terms, is constrained by the form of the superpotential which, in turn, is generally constrained by local and global symmetries.

III. TREE-LEVEL AND RADIATIVE CONTRIBUTIONS TO THE QUARK MASS MATRIX

The quark mass matrix (up or down) is given by

$$\begin{array}{c} \\ q_i \\ q' \\ q_i^{c*} \\ q'^{c*} \end{array} \begin{array}{c} \begin{array}{cccc} q_i^* & q'^* & q_i^c & q'^c \end{array} \\ \begin{pmatrix} & & & \\ 0 & \cdots & M & \\ \vdots & & \vdots & \\ & & & \\ M^+ & \cdots & 0 & \end{pmatrix} \end{array} . \tag{3.1}$$

The quark masses and eigenstates are found by solving the eigenvalue equations

$$MM^\dagger|\Psi_L\rangle = m^2|\Psi_L\rangle, \quad M^\dagger M|\Psi_R\rangle = m^2|\Psi_R\rangle , \tag{3.2}$$

where the bases for $|\Psi_L\rangle$ and $|\Psi_R\rangle$ are

$$(q_i q') \text{ and } (q_i^{c*} q'^{c*}) , \tag{3.3}$$

respectively. The eigenstates $|\Psi_L\rangle$ and $|\Psi_R\rangle$ are related via

$$|\Psi_R\rangle = \frac{M^\dagger}{m}|\Psi_L\rangle . \tag{3.4}$$

M is given by

$$M = M^0 + M^1 . \tag{3.5}$$

M^0, which originates at the tree level, leads to mirror and third family quark masses, to be discussed presently. M^1 consists of radiative contributions to the quark mass matrix which generate the quark mixing hierarchy and light-quark masses. Their origin is discussed in Sec. III B.

A. Tree-level quark masses

The mass matrix M^0 is given by

$$M^0 = \begin{pmatrix} 0 & a_L|h_L\rangle \\ a_R\langle h_R| & M' \end{pmatrix} , \tag{3.6}$$

$\langle h_R|$ and $|h_L\rangle$ are three-component row and column vectors. At the tree level the above entries are related to the couplings and VEV's of (2.2)–(2.7) as

$$\begin{aligned} a_L &= \langle\rho\rangle \left[\sum |h_{Li}|^2\right]^{1/2} , \\ a_R &= \langle\rho\rangle \left[\sum |h_{Ri}|^2\right]^{1/2} , \\ |h_L\rangle &= h_{Li} / \left[\sum |h_{Li}|^2\right]^{1/2} , \\ |h_R\rangle &= h^*_{Ri} / \left[\sum |h_{Ri}|^2\right]^{1/2} , \\ M'_u &= \lambda_1\langle\tilde{N}_E\rangle, \quad M'_d = \lambda_1\langle\tilde{\nu}_E\rangle . \end{aligned} \tag{3.7}$$

Note that $|h_L\rangle, |h_R\rangle^{u,d}$ are normalized to unity. There will also be radiative gaugino-squark graph contributions to $a_{L,R}$, M', and these are absorbed into (3.6). $SU(2)_L$ invariance implies $a_L^u = a_L^d$, while $SU(2)_R$ invariance would further imply $a_R^u = a_R^d$ and $\lambda_1^u = \lambda_1^d$. Diagonalization of $M^0 M^{0\dagger}$ yields four orthonormal left-handed eigenstates: $|1_L\rangle, |2_L\rangle$ are massless and correspond to the first and second families, while $|3_L\rangle, |4_L\rangle$ are massive and correspond to the third and mirror families, respectively. The nonzero masses and corresponding eigenstates are given by

$$\begin{aligned} m_k^2 &= \tfrac{1}{2}\{(a_L^2 + a_R^2 + M'^2) \mp [(a_L^2 + a_R^2 + M'^2)^2 \\ &\qquad - 4a_L^2 a_R^2]^{1/2}\} \\ |k_L\rangle &= \frac{1}{(N_{Lk})^{1/2}} \begin{pmatrix} c_{Lk}|h_L\rangle \\ 1 \end{pmatrix}, \quad N_{Lk} = c_{Lk}^2 + 1 , \\ c_{Lk} &= \frac{a_L}{m_k^2 M'}(m_k^2 - a_R^2), \quad k = 3,4 , \end{aligned} \tag{3.8}$$

where m_3^2, m_4^2 correspond to subtraction, addition, respectively, in (3.8). Note that m_3, m_4 satisfy

$$m_3^2 m_4^2 = a_L^2 a_R^2, \quad m_3^2 \le m_4^2 , \tag{3.9}$$

with equality in the second relation possible when $M' = 0$. The choice of $|1_L\rangle, |2_L\rangle$ depends on the form of the mass contributions contained in M^1 and is dictated by convenience in carrying out the associated perturbative calculation of light-quark masses, cf. Sec. IV. Using (3.4) the corresponding orthonormal massive right-handed eigenstates are found to be

$$\begin{aligned} |k_R\rangle &= \frac{1}{(N_{Rk})^{1/2}} \begin{pmatrix} c_{Rk}|h_R\rangle \\ 1 \end{pmatrix} , \\ c_{Rk} &= \frac{a_R^*}{m_k^2 M'^*}(m_k^2 - a_L^2), \quad k = 3,4 . \end{aligned} \tag{3.10}$$

The effects of M^1 can be regarded as a perturbation to the

above results and one makes the following identification of quark masses:

$$m_b = m_3^d + m_b^{\rm rad},\ m_{t_3} = m_3^u + m_{t_3}^{\rm rad} \sim m_3^u\ ,$$
$$m_{b'} = m_4^d + m_{b'}^{\rm rad} \sim m_4^d,\ \ m_{t_4} = m_4^u + m_{t_4}^{\rm rad} \sim m_4^u\ , \tag{3.11}$$

where m_b, $m_{b'}$ are the ordinary-bottom and mirror-bottom-quark masses, respectively, while m_{t_3}, m_{t_4} are the masses of the two top quarks. As indicated, radiative contributions are of significance for m_b, cf. Sec. III B 2.

In the limit $M' \gg a_L, a_R$, which is referred to as the seesaw limit, (3.8) reduces to

$$m_3^2 \sim \left[\frac{a_L a_R}{M'}\right]^2,\ \ m_4^2 \sim M'^2\ ,$$
$$|3_L\rangle \sim \begin{bmatrix} -|h_L\rangle \\ a_L/M' \end{bmatrix},\ \ |4_L\rangle \sim \begin{bmatrix} (a_L/M')|h_L\rangle \\ 1 \end{bmatrix}. \tag{3.12}$$

The seesaw limit will be valid for the down quarks since m_b must be seesaw suppressed due to its small value [see Table III(b) for explicit examples]. However, $m_{t_{3,4}} \gg m_b$ requires $M'_d \gg M'_u$, or $\langle \nu_E \rangle \gg \langle N_E \rangle$ if $\lambda_{1d} \sim \lambda_{1u}$ as in left-right-symmetric models. The seesaw limit is therefore not expected to be valid for the up-quark sector and the full expressions (3.8) must be used to determine $m_{t_{3,4}}$ and the corresponding eigenstates. Because of the absence of seesaw suppression the two top quarks will have similar masses and both will have large $V-A$ as well as $V+A$ couplings to the ordinary Z [see Table III(a) for explicit examples]. The ordinary top is defined to be the one with large $V-A$ coupling [satisfying $|c_{Lk}/(N_{Lk})^{1/2}| > 1/(N_{Rk})^{1/2}$] and is not necessarily the lighter of the two. Absence of seesaw suppression leads to large flavor-changing neutral-current (FCNC) effects in the up sector, cf. Sec. VI.

As remarked above, we require $M'_d \gg M'_u$ or, equivalently, $m_{b'} \gg m_{t_{3,4}}$. However, because mirror quarks are isodoublets of $SU(2)_L$ this mass splitting is bounded from above due to radiative corrections to the ρ parameter.[9] Contributions to the ρ parameter due to superpartners can be neglected since we will be considering the limit where their isodoublet mass splitting is much smaller than their characteristic mass scale.[15] Because both t_3 and t_4 are expected to have large admixtures of u'^c [see Tables I and III(a)] we require

$$|m_{b'\rm phys}| - |m_{t_{3,4}\rm phys}| \lesssim 200\text{–}300\ {\rm GeV}\ , \tag{3.13}$$

corresponding to $\delta\rho \lesssim 0.01\text{–}0.03$. For the left-right-symmetric case G_{LR} or, more generally, for models without explicit isospin breaking in the superpotential, because $a_R^u = a_R^d$, Eq. (3.9) implies

$$m_3^d m_4^d = m_3^u m_4^u\ . \tag{3.14}$$

Equations (3.13) and (3.14) together imply an upper bound for m_{t_3}. From (3.11), (3.13), and (3.14) one obtains

$$|m_{b'\rm phys}| - |m_{t_4\rm phys}| \sim |m_{t_4}(1\ {\rm GeV})| \left[\left|\frac{m_{t_3}}{m_3^d}(1\ {\rm GeV})\right|^{0.5\text{–}0.6}\right], \tag{3.15}$$

where the factors 0.5, 0.6 (obtained from extrapolation of results of Ref. 1) account, approximately, for QCD running of quark masses from 1 GeV to 200–300, 30–50 GeV, respectively. The upper bound on m_{t_3} is then obtained by setting $m_{t_4} = m_{t_3}$ in (3.15), see (3.9). Taking $|m_b(1\ {\rm GeV})| = 5.3$ GeV, corresponding to $\Lambda_{\rm QCD} = 100$ MeV (Ref. 1) and neglecting $m_b^{\rm rad}$ leads to the bound

$$m_{t_3\rm phys} \lesssim 30\text{–}35\ {\rm GeV}\ . \tag{3.16}$$

Radiative contributions to m_b can increase the upper bound slightly. For example, if $|m_b^{\rm rad}(1\ {\rm GeV})| \sim 3$ GeV (such a value is readily attainable, cf. Sec. III B 2), and $\mathrm{sgn}(m_b^{\rm rad}) = -\mathrm{sgn}(m_b)$ [see (3.11)], m_3^d can be increased in magnitude by the same amount and the upper bound is raised to 37–43 GeV. Note, also, that QCD running of fermion masses changes significantly as $\Lambda_{\rm QCD}$ is varied. Despite the large uncertainties involved, it is clear that for the left-right-symmetric case ρ parameter constraints force a light top-quark scenario. Although probably ruled out experimentally by UA1, a numerical illustration of this case is included in Table III (see example 1) for completeness. Note that physical quark masses in Table III are only approximate. Reliable estimates require a careful calculation of QCD running of masses and should also take into account possible variations in $\Lambda_{\rm QCD}$. Of course, for non-left-right-symmetric choices of $G_{\rm EW}$, since a_R^u and a_R^d need not be equal relation (3.14) will not apply in general and is, in fact, replaced by $|m_3^d m_4^d| = |\alpha m_3^u m_4^u|$ where $\alpha = |a_R^d/a_R^u|$. Consequently, the above upper limit on m_{t_3} can be evaded; however this requires explicit isospin breaking in the Yukawa sector, i.e., $|a_R^u| > |a_R^d|$ or $\alpha < 1$. For numerical illustrations of this case, featuring $m_{t_3\rm phys} \sim 53$, 79 GeV, see Table III, examples 2 and 3, respectively. Again, radiative contributions to m_b allow accommodation of larger top-quark mass. Approximate upper bounds on m_{t_3} (only intended as a guideline) can be obtained from the appropriate generalization of (3.15). For example, taking $|m_{b'\rm phys}| - |m_{t_4\rm phys}| \lesssim 200$ GeV, $m_3^d = 6$ GeV, and $\alpha = 0.2, 0.1$ leads to $m_{t_3\rm phys} \lesssim 77$, 117 GeV, respectively (the extrema obtain when $m_{t_3} = m_{t_4}$) corresponding to upper bounds on $m_{b'\rm phys}$ of order 300 GeV. Detailed numerical work taking full account of QCD evolution is required in order to obtain more precise bounds.

For models without explicit isospin breaking in the superpotential (this is an attractive feature which further reduces reliance on Yukawa coupling hierarchies) of which G_{LR} is a special case, a large top-quark mass $\sim 50\text{–}100$ GeV, can be accommodated if the field content includes a light pair of isosinglet down quarks D, D^c which mixes exclusively with the mirror down quarks. (If they also mixed with ordinary down quarks two ordinary down quarks would pick up mass at the tree level, spoil-

TABLE III. (a) and (b) contain numerical illustrations of third, mirror family up- and corresponding down-quark masses and eigenstates, respectively. $G_{LR}=\mathrm{SU}(2)_L\otimes\mathrm{SU}(2)_R\otimes\mathrm{U}(1)_{B-L}$, $G_{1R}=\mathrm{SU}(2)_L\otimes\mathrm{U}(1)_R\otimes\mathrm{U}(1)_{B-L}$, $G_{1Y}=\mathrm{SU}(2)_L\otimes\mathrm{U}(1)_Y$. In examples 1, 2, and 3, $m_b^{\mathrm{rad}}\sim 0$, 0, 0.7 GeV, respectively. Physical top and mirror bottom mass entries, obtained from their values at 1 GeV by multiplying the latter by 0.6 and 0.5, respectively, are approximate and only intended as a guideline.

	Example 1 (G_{LR})	Example 2 (G_{1R} or G_{1Y})	Example 3 (G_{1R} or G_{1Y})
		(a)	
$a_L(1\ \mathrm{GeV})$	55 GeV	100 GeV	137 GeV
$a_R^u(1\ \mathrm{GeV})$	55 GeV	90 GeV	137 GeV
$M_u'(1\ \mathrm{GeV})$	11 GeV	10 GeV	10 GeV
$m_{t_3\mathrm{phys}}$	~ -30 GeV	~ -53 GeV	~ -79 GeV
$m_{t_4\mathrm{phys}}$	~ 36 GeV	~ 61 GeV	~ 85 GeV
$\lvert\psi_{3L}^u\rangle$	$\begin{bmatrix} -0.72\lvert h_L\rangle \\ 0.69 \end{bmatrix}$	$\begin{bmatrix} -0.42\lvert h_L\rangle \\ 0.91 \end{bmatrix}$	$\begin{bmatrix} -0.72\lvert h_L\rangle \\ 0.69 \end{bmatrix}$
$\lvert\psi_{4L}^u\rangle$	$\begin{bmatrix} 0.69\lvert h_L\rangle \\ 0.72 \end{bmatrix}$	$\begin{bmatrix} 0.91\lvert h_L\rangle \\ 0.42 \end{bmatrix}$	$\begin{bmatrix} 0.69\lvert h_L\rangle \\ 0.72 \end{bmatrix}$
$\lvert\psi_{3R}^u\rangle$	$\begin{bmatrix} -0.72\lvert h_R\rangle \\ 0.69 \end{bmatrix}$	$\begin{bmatrix} -0.93\lvert h_R^u\rangle \\ 0.36 \end{bmatrix}$	$\begin{bmatrix} -0.72\lvert h_R\rangle \\ 0.69 \end{bmatrix}$
$\lvert\psi_{4R}^u\rangle$	$\begin{bmatrix} 0.36\lvert h_R\rangle \\ 0.72 \end{bmatrix}$	$\begin{bmatrix} 0.36\lvert h_R\rangle \\ 0.93 \end{bmatrix}$	$\begin{bmatrix} 0.69\lvert h_R\rangle \\ 0.72 \end{bmatrix}$
		(b)	
$a_L(1\ \mathrm{GeV})$	55 GeV	100 GeV	137 GeV
$a_R^d(1\ \mathrm{GeV})$	55 GeV	17 GeV	23 GeV
$M_d'(1\ \mathrm{GeV})$	545 GeV	300 GeV	500 GeV
m_3^d 1 GeV)	-5.5 GeV	-5.4 GeV	-6.3 GeV
$m_{b\ \mathrm{phys}}'$	~ 275 GeV	~ 160 GeV	~ 259 GeV
$\lvert\psi_{3L}^d\rangle$	$\begin{bmatrix} -0.99\lvert h_L\rangle \\ 0.1 \end{bmatrix}$	$\begin{bmatrix} -0.95\lvert h_L\rangle \\ 0.32 \end{bmatrix}$	$\begin{bmatrix} -0.96\lvert h_L\rangle \\ 0.26 \end{bmatrix}$
$\lvert\psi_{4L}^d\rangle$	$\begin{bmatrix} 0.1\lvert h_L\rangle \\ 0.99 \end{bmatrix}$	$\begin{bmatrix} 0.32\lvert h_L\rangle \\ 0.95 \end{bmatrix}$	$\begin{bmatrix} 0.26\lvert h_L\rangle \\ 0.96 \end{bmatrix}$
$\lvert\psi_{3R}^d\rangle$	$\begin{bmatrix} -0.99\lvert h_R\rangle \\ 0.1 \end{bmatrix}$	$\begin{bmatrix} -0.99\lvert h_R^d\rangle \\ 0.05 \end{bmatrix}$	$\begin{bmatrix} -0.99\lvert h_R^d\rangle \\ 0.04 \end{bmatrix}$
$\lvert\psi_{4R}^d\rangle$	$\begin{bmatrix} 0.1\lvert h_R\rangle \\ 0.99 \end{bmatrix}$	$\begin{bmatrix} 0.05\lvert h_R^d\rangle \\ 0.99 \end{bmatrix}$	$\begin{bmatrix} 0.04\lvert h_R^d\rangle \\ 0.99 \end{bmatrix}$

ing the hierarchy.) This will be reported on elsewhere.[16] We only note here that the additional isosinglet quarks alter relation (3.14) since in this case there would be three massive down-quark eigenstates at the tree level. As a result, small upper bounds on m_{t_3} obtained for the ordinary left-right-symmetric case can again be evaded. The desired vacuum alignment in this case, however, differs from that of (2.7) with $SU(2)_L$ broken primarily via $\langle \nu'^c \rangle$.

B. The radiative scheme

The matrix M^1, which consists of radiative contributions to the quark mass matrix (3.5), is of the form

$$M^1 = \begin{bmatrix} \delta M & 0 \\ 0 & 0 \end{bmatrix} . \tag{3.17}$$

δM is a 3×3 matrix. Recall that radiative entries along the last row and column have been absorbed into M^0. The dominant radiative contribution to δM involve squark propagation in the loops. It is therefore necessary to begin with discussion of the tree-level squark mass matrix $\tilde{M}_q^2$ ($q = u$ or d), given by

$$\tilde{M}_q^2 = \begin{array}{c} \\ \tilde{q}_i \\ \tilde{q}' \\ \tilde{q}_i^{c*} \\ \tilde{q}'^{c*} \end{array} \begin{array}{c} \begin{array}{cccc} \tilde{q}_i^* & \tilde{q}'^* & \tilde{q}_i^c & \tilde{q}'^c \end{array} \\ \begin{bmatrix} M_L^2 & \chi_L^2 |h_L\rangle & 0 & \mu_L^2 |\tilde{h}_L\rangle \\ \chi_L^{2*}\langle h_L| & m_R'^2 & \mu_R^2 \langle \tilde{h}_R| & \mu'^2 \\ 0 & \mu_R^{2*}|\tilde{h}_R\rangle & M_R^2 & \chi_R^{2*}|h_R\rangle \\ \mu_L^{2*}\langle \tilde{h}_L| & \mu'^{2*} & \chi_R^2 \langle h_R| & m_L'^2 \end{bmatrix} \end{array} . \tag{3.18}$$

The above entries are given below in terms of the couplings and VEV's of (2.3)–(2.7).

Down squarks ($q = d$):

$$\begin{aligned}
&M_{Rij}^2 = m_{\tilde{d}^c ij}^2 + |h_{Ri}|^2\delta_{ij} + D^2 \text{ terms} , \quad M_{Lij}^2 = m_{\tilde{d}ij}^2 + |h_{Li}|^2\delta_{ij} + D^2 \text{ terms} , \\
&m_R'^2 = m_{\tilde{d}'}^2 + |M_d'|^2 + |a_R|^2 + D^2 \text{ terms} , \quad m_L'^2 = m_{\tilde{d}'^c}^2 + |M_d'|^2 + |a_L|^2 + D^2 \text{ terms} , \\
&\chi_{L,(R)}^2 = a_{L,(R)} M_d'^* , \quad \mu'^2 = A_1 \langle \tilde{\nu}_E \rangle + \lambda_1 \lambda_4^* \langle \tilde{y} \rangle^* \langle \tilde{N}_E \rangle^* , \\
&\mu_{L,(R)}^2 = \left[\sum_i | A_{L,(R)i}^Q \langle \tilde{\rho} \rangle + h_{L,(R)i} (\lambda_R^* \langle \tilde{N}^c \rangle^* \langle \tilde{N}' \rangle^* + \lambda_3^* \langle \tilde{\rho} \rangle^{2*} + \mu^* \langle \tilde{y} \rangle^*) |^2 \right]^{1/2} , \\
&|\tilde{h}_{L,(R)}\rangle_i = [A_{L,(R)i}^Q \langle \tilde{\rho} \rangle + h_{L,(R)i} (\lambda_R^* \langle \tilde{N}^c \rangle^* \langle \tilde{N}' \rangle^* + \lambda_3^* \langle \tilde{\rho} \rangle^{2*} + \mu^* \langle \tilde{y} \rangle^*)]^{(*)} / \mu_{L,(R)}^2 .
\end{aligned} \tag{3.19a}$$

Up squarks ($q = u$):

$$\begin{aligned}
&M_{Rij}^2 = m_{\tilde{u}^c ij}^2 + |h_{Ri}|^2\delta_{ij} + D^2 \text{ terms} , \\
&M_{Lij}^2 = m_{\tilde{u}ij}^2 + |h_{Li}|^2\delta_{ij} + D^2 \text{ terms} , \\
&m_R'^2 = m_{\tilde{u}'}^2 + |M_u'|^2 + |a_R|^2 + D^2 \text{ terms} , \\
&m_L'^2 = m_{\tilde{u}'^c}^2 + |M_u'|^2 + |a_L|^2 + D^2 \text{ terms} , \\
&\chi_{L,(R)}^2 = a_{L,(R)} M_u'^* , \\
&\mu'^2 = A_1 \langle \tilde{N}_E \rangle + \lambda_1 \lambda_4^* \langle \tilde{y} \rangle^* \langle \tilde{\nu}_E \rangle^* \\
&\qquad + \lambda_1 \lambda_2^* \langle \tilde{\nu}'^c \rangle^* \langle \tilde{N}' \rangle^* , \\
&\mu_{L,R}^2 |\tilde{h}_{L,R}\rangle_i \text{ same as above} .
\end{aligned} \tag{3.19b}$$

Bras and kets are again normalized to unity. All terms above containing A or $m_{\tilde{\phi}_i}$ parameters (where A is any scalar trilinear coupling and $\tilde{\phi}_i$ is any scalar in the theory) originate in V_{soft} (2.6) while the remaining terms shown explicitly originate in the F^2 sector of the scalar potential. The largest D^2 contributions, given in magnitude by $(g_R^2/8)||\langle \tilde{N}^c \rangle|^2 - |\langle \tilde{N}' \rangle|^2|$ and $(g_{B-L}^2 |Q_{B-L}|/4)||\langle \tilde{N}^c \rangle|^2 - |\langle \tilde{N}' \rangle|^2|$ (Q_{B-L} is the $B-L$ charge of the corresponding squark) occur in $M_{ii}^2, m_R'^2$ and correspond to $SU(2)_R$ or $U(1)_R$ and $U(1)_{B-L}$, respectively. Remaining D^2 contributions are of similar form but involve squares of $SU(2)_L$-breaking VEV's. Of course for G_{1Y} there are no D^2 terms involving $\langle \tilde{N}^c \rangle$, $\langle \tilde{N}' \rangle$. The 3×3 submatrices M_L^2, M_R^2, expected to be diagonal and degenerate at the scale at which they are generated (M_P in minimal supergravity) will not remain so, in general, at low energy due to renormalization-group effects as well as contributions of F^2 terms [see (3.19)]. The extent of this will be of relevance to our discussion and we return to this point shortly.

The one-loop squark exchange graphs are of two types: those with isosinglet down squarks D, D^c and those with gauginos in the loop. We begin with the former, which in our scheme are expected to generate the bulk of m_c, m_s.

1. *One-loop squark, isosinglet quark graphs*

The isosinglet quarks D, D^c form a Dirac fermion with mass μ_D [see (2.4)] which propagates inside these graphs. There will be many such graphs contributing to $\delta M^{u,d}$ corresponding to different numbers of occurrences of the mass insertions $\mu_{L,R}^2, \chi_{L,R}^2, \mu'^2$ along the internal squark line. Diagrams with $\chi_{L,R}^2$ mass insertions can be neglected since $\chi_{L,R}^2 \ll \mu_{L,R}^2, \mu'^2$ for $\langle N^c \rangle$, $\langle N' \rangle$, $A_1 \sim 10^3 - 10^4$ GeV [see (2.7), (3.19), and examples of Tables III]. The simplest graphs to consider are Fig. 2 contributing to δM^u and its analogue contributing to δM^d, in which the mass insertions $\mu_{L,R}^2, \mu'^2$ each appear only once. Although we will be considering the limit where $\mu_{L,R}^2 \sim m_{L,R}'^2, M_{L,Rii}^2$, Fig. 2 provides an order-of-magnitude estimate of the total contribution of this class of graphs to δM and is also useful for illustrating under

what conditions the observed hierarchy between first- and second-generation masses will obtain. The exact calculation of δM due to this class of graphs, equivalent to summing over graphs with any number of mass insertions, is tedious as one must first diagonalize $\tilde{M}_q^2$ and then sum over all graphs contributing to δM, each with a different squark mass eigenstate in the loop. Such a calculation is presented in the Appendix in the limit where $\tilde{M}_q^2$ is invariant under P (parity) and M_L^2, M_R^2 are diagonal and degenerate. $\tilde{M}^2$ is straightforward to diagonalize in this case. A comparison with results of the Appendix suggests that the contribution of Fig. 2, although large is within a factor of 2–3 of the exact result. We begin by showing that the contributions of Fig. 2 and its down-quark analogue (and, therefore, the total contribution of this class of graphs) can easily be at the level of m_c and m_s, respectively.

Before proceedings with discussion of Fig. 2 we set the notation for the eigenstates and eigenvalues of $M_{L,R}^2$ in (3.18):

for M_L^2, the eigenstates are $|\tilde{k}_L\rangle$

$$\text{with mass } m_{kL}^2, k=1,2,3 , \tag{3.20}$$

for M_R^2, the eigenstates are $|\tilde{j}_R\rangle$

$$\text{with mass } m_{jR}^2, j=1,2,3 .$$

The contribution of Fig. 2 and its d-quark analogue to $\delta M^{u,d}$, denoted by $\delta M_D^{u,d}$, is then given by

$$\delta M_D^{u,(d)} = \left[\sum_{j,k} H^L |\tilde{k}_L\rangle\langle\tilde{k}_L| (|\tilde{h}_L\rangle\langle\tilde{h}_R|)^* \times |\tilde{j}_R\rangle\langle\tilde{j}_R| H^R a_D^{u,(d)}(m_{jR}^2, m_{kL}^2) \right] , \tag{3.21}$$

where

$$a_D^{u,(d)}(m_{jR}^2, m_{kL}^2) = F_c [\mu_L^{2*}\mu_R^{2*}\mu'^2\mu_D^* I(m_{jR}^2, m_{kL}^2, m_L'^2, m_R'^2, \mu_D^2)]_{\tilde{d},(\tilde{u})} . \tag{3.22}$$

$I(m_{jR}^2, m_{kL}^2, m_L'^2, m_R'^2, \mu_D^2)$ are just the loop integrals and F_c is a color factor, $F_c=2$. The subscript $\tilde{d}$ ($\tilde{u}$) indicates that down- (up-) squark mass matrix parameters (3.19) should be understood in the brackets. Note that the exact result can be cast in the same form as (3.21) although expressions for the massive a_D parameters will be changed.

In general,

$$m_{jR}^2 \sim m_{kL}^2 \sim m^2, \quad m_L'^2 \sim m_R'^2 \sim m'^2, \quad m^2 \sim m'^2 \sim m_{\text{SUSY}}^2 , \tag{3.23}$$

where m_{SUSY} is the scale of soft SUSY-breaking terms, $\sim$1–10 TeV. In the limit where $m_{jR}^2 = m_{kL}^2 = m^2$, $m_L'^2 = m_R'^2 = m'^2$, I is given by

$$I = \frac{1}{16\pi^2} \left\{ \frac{1}{(m^2-m'^2)^2} \left[\ln\frac{\mu_D^2}{m'^2} \left[\frac{\mu_D^2}{(m'^2-\mu_D^2)^2} + \frac{2m'^2}{(m^2-m'^2)(\mu_D^2-m'^2)} \right] + \ln\frac{\mu_D^2}{m^2} \left[\frac{\mu_D^2}{(m^2-\mu_D^2)^2} + \frac{-2m^2}{(m^2-m'^2)(\mu_D^2-m^2)} \right] \right] + \frac{1}{m'^2-\mu_D^2} + \frac{1}{m^2-\mu_D^2} \right\} . \tag{3.24}$$

Taking $\mu_D \sim m$, Eqs. (3.22), (3.23), and (3.24) together imply

$$a_D^{u,(d)} \sim \frac{F_c=2}{16\pi^2} \left[\frac{\mu_L^2\mu_R^2\mu'^2}{m^5} \right]_{\tilde{d},(\tilde{u})} . \tag{3.25}$$

A comparison with results of the Appendix suggests this estimate is too large but within a factor of 2–3 of the exact calculation (summing over all squark mass eigenstates in the loop) of δM_D. An upper bound for a_D^q is obtained from (3.25) via the squark mass inequalities given below, which follow from requiring color conservation (the second inequality is approximate):

$$m_L'^2 + m_R'^2 + m_{\tilde{\phi}}^{2\,\text{tot}} \gtrsim A_1^2/3\lambda_1^2, \quad m^2 m'^2 \gtrsim \mu_{L,R}^4 . \tag{3.26}$$

$m_{\tilde{\phi}}^{2\,\text{tot}}$ is the total scalar mass of the appropriate component of $\tilde{\phi}$. From (3.19) and (2.7) it follows that the second inequality can readily be saturated. Assuming validity of (3.23) and $m_{\tilde{\phi}}^{2\,\text{tot}} \lesssim m^2$, one obtains

$$\mu_d'^2 \lesssim (2.5-3) m M_d' \sim m\, 10^3 \text{ GeV}^2 , \tag{3.27}$$

from (3.19), (2.7), Table III(b), and the first inequality in (3.26). Equations (3.25)–(3.27) in turn imply

$$a_D^u \lesssim 13 \text{ GeV} . \tag{3.28}$$

From results of the Appendix this bound is probably too large but within a factor of 2–3 of the correct upper bound. In the non-left-right case [see examples 2 and 3 of Table III(b)] the upper limit will be suppressed by a factor $\mu_R^{2d}/\mu_L^2 \sim a_R^d/a_L$. Nevertheless, since Yukawa couplings are $\sim$1 it is clear that m_c can easily be generated radiatively. We return to discussion of the couplings shortly.

The inequality $\langle N_E \rangle \ll \langle \nu_E \rangle$ (or $M_u' \ll M_d'$) will lead to $\mu_{\tilde{u}}'^2 \ll \mu_{\tilde{d}}'^2$, provided $\lambda_4\langle y\rangle \ll A_1$, see (3.19). However, for $A_1 \lesssim (2.5-3)\lambda_1 m$, (3.27), and $m \sim$1–10 TeV, this relation can readily be satisfied. As a result one expects $a_D^d \ll a_D^u$ or $m_s \ll m_c$ as is observed [see (3.25)]. The fact that D, D^c are charged is crucial for this result. The above VEV (or mirror quark mass) inequality, obtained without the need for explicit isospin breaking in the superpotential, can therefore account for both $m_t \gg m_b$ and $m_c \gg m_s$. We will see (cf. Secs. III B 2 and III B 3) that it can lead to $m_d \gtrsim m_u$ as well.

In general $\delta M_D^{u,d}$ will be rank-three matrices (3.21) and a mass hierarchy between first- and second-generation quarks will not obtain. To avoid this M_L^2, M_R^2 must each be degenerate (the validity of this assumption within the context of supergravity models is briefly discussed below) at the 10% level or less. Their eigenvalues can then be written as

$$m_{jL,R}^2 = m_{L,R}^2 + \delta m_{jL,R}^2 , \tag{3.29}$$

where

$$(\delta m_j^2/m^2)_{L,R} \lesssim 0.1 . \tag{3.30}$$

Taylor expanding about $m_{L,R}^2$, δM_D^q can be written as

$$\delta M_D^{u,(d)} = [a_D^{u,(d)}(m_R^2, m_L^2) H^L (|\tilde{h}'_L\rangle\langle \tilde{h}'_R|)^* H^R]_{\bar{d},(\bar{u})} + \delta_3 M_D^{u,(d)} , \tag{3.31}$$

where $\delta_3 M_D^q$ is a rank-three matrix *which is suppressed by a factor* $(\delta m_j^2/m^2)^2$ relative to the first term, which is a rank-one matrix. In the first term

$$|\tilde{h}'_R\rangle = |\tilde{h}_R\rangle + \sum_j [a_{jR}^D / a_D(m_R^2, m_L^2)]^* |\tilde{j}_R\rangle\langle \tilde{j}_R|\tilde{h}_R\rangle ,$$
$$|\tilde{h}'_L\rangle = |\tilde{h}_L\rangle + \sum_k [a_{k_L}^D / a_D(m_R^2, m_L^2)]^* |\tilde{k}_L\rangle\langle \tilde{k}_L|\tilde{h}_L\rangle , \tag{3.32}$$

and

$$a_{jR,L}^D = \left[\delta m_j^2 \frac{\partial a_D}{\partial m^2}(m_R^2, m_L^2)\right]_{R,L} \sim \left[\frac{\delta m_j^2}{m^2}\right]_{R,L} a_D . \tag{3.33}$$

Validity of (3.30) ensures that if the rank-one piece in (3.31) is at the level of second-generation quark masses then the rank-three piece is less than or at the level of first-generation quark masses. It is not difficult to see that validity of (3.30) implies that the total contribution of this class of graphs can also be written in the form (3.31) [of course expressions for the various quantities in (3.31) will differ] with the same order suppression between the first and second terms thus allowing for the observed mass hierarchy between first- and second-generation quarks.

The first term in (3.31) rewritten in terms of normalized bra and ket is given by

$$\tilde{a}^q_{\bar{b}} |\tilde{H}\tilde{h}'_L\rangle\langle \tilde{H}\tilde{h}'_R| , \tag{3.34}$$

where

$$\tilde{a}^q_{\bar{b}} = a_{\bar{b}}^q(m_R^2, m_L^2)\sqrt{n_L}\sqrt{n_R} ,$$
$$n_L = (\langle \tilde{h}'_L|)^* H^{L\dagger} H^L (|\tilde{h}'_L\rangle)^* , \tag{3.35}$$
$$n_R = (\langle \tilde{h}'_R|)^* H^R H^{R\dagger} (|\tilde{h}'_R\rangle)^* .$$

Comparing with (3.28) and results of the Appendix one requires n_L, $n_R \sim 1$ to obtain m_c at the observed level. The inequality $M'_d \gg M'_u$ will imply $m_c \gg m_s$ as well as $\delta_3 M_D^u \gg \delta_3 M_D^d$ so contributions of Fig. 2 to first-generation quark masses are expected to be larger for the up quark.

Lower bounds can be derived for m (the ordinary squark mass scale), $m_{\tilde{g}}$, μ_D, and $m^2_{\tilde{D},\tilde{D}^c}$ in various combinations from K-$\bar{K}$ box graphs[17] which contain these particles in the loops. The dominant graphs contain both left-handed (LH) and right-handed (RH) quarks along the external legs. For example, from ΔM_K, gluino-ordinary squark graphs lead to the constraint

$$\frac{1}{\max(m^2, m_{\tilde{g}}^2)} \left[\frac{\delta m_j^2}{m^2}\right]_L \left[\frac{\delta m_j^2}{m^2}\right]_R \lesssim 10^{-9}-10^{-10} .$$

Comparing with the above, isosinglet-quark–ordinary-squark graphs yield

$$\frac{1}{\max(m^2, \mu_D^2)} \frac{H_{ij}^{L2} H_{ij}^{R2}}{g_{\rm QCD}^4} \lesssim 10^{-9}-10^{-10} .$$

A safe mass scale for all of these parameters turns out to be ~ 5–10 TeV, implying a large supersymmetry-breaking scale. In making this determination, we have assumed $(\delta m_j^2/m^2)_{L,R} \sim 10^{-1}$, and taken $H_{ij}^{L,R} \sim \frac{1}{3}$ (which, for $\tilde{h}'_{L,Ri} \sim 1/\sqrt{3}$, corresponds to $n_{L,R} \sim 1$).

Next we wish to comment on validity of the degeneracy assumption (3.30) within the context of supergravity theories. Changes in $M_{L,R}^2$, initially diagonal and degenerate, due to renormalization-group evolution down to low energies are schematically given by

$$\Delta M_{L,R}^2 \sim \frac{1}{4\pi^2} \ln\left[\frac{M_i}{m}\right] [2m^2 (H^\dagger H)^{L,R} + (A^{H\dagger} A^H)^{L,R}] - \frac{1}{2\pi^2} \ln\left[\frac{M_i}{m_{\tilde{g}}}\right] \frac{4}{3} m_{\tilde{g}}^2 g_{\rm QCD}^2 I + \text{electroweak interactions} , \tag{3.36}$$

where M_i ($\sim M_P$ in minimal supergravity) is the scale at which soft SUSY-breaking terms arise, m is the initial scalar mass scale, and $m_{\tilde{g}}$ ($\sim m$ in minimal supergravity) is the gluino mass. [Effects of F^2 terms are negligible in this regard because $a_{L,R} \ll m_{\rm SUSY}$, see (3.19), Table III.] Bearing in mind that within our scheme low-energy entries in $(H^\dagger H)^{L,R}$ should typically be $\sim \frac{1}{3}$, corresponding to $n_{L,R} \sim 1$ (a requirement for radiative generation of m_c), it is apparent from (3.36) that near degeneracy of $M_{L,R}^2$ (3.30) is unobtainable within the context of minimal supergravity due to the Yukawa and scalar trilinear interactions. However, if QCD is asymptotically divergent, as in MPP unification[11] (cf. Sec. VII) then gauge interactions (QCD in particular), which are flavor diagonal and contribute positively in (3.36), become very important and can help our cause. Furthermore, in alternative formulations of supergravity it is possible that initially $m_{\rm gaugino} \gg m, A^H$. In fact in no-scale supergravity,[18] believed to be the low-energy effective theory resulting from the superstring m and A^H would initially be ~ 0. In this case gauge interactions could dominate the renormalization-group evolution, especially if QCD is

asymptotically divergent. Numerical investigation of these issues is certainly of interest.

At the other extreme, if M_L^2, M_R^2 are not degenerate at low energies the desired mass hierarchy between first- and second-generation quarks will obtain if first-generation current quarks are decoupled from the remaining quarks by an order of magnitude in $H^{L,R}, h_{L,R}$, i.e., if all Yukawa couplings involving q_1^c are suppressed by an order of magnitude. This will also lead to decoupling for the corresponding squarks in $M_{L,R}^2$ at low energies, e.g., $\langle \tilde{q}_1 | M_L^2 | \tilde{q}_j \rangle \sim 10^{-1} (\langle \tilde{q}_1 | M_L^2 | \tilde{q}_1 \rangle, \langle \tilde{q}_i | M_L^2 | \tilde{q}_k \rangle)$, $i,j,k=2,3$ due to decoupling in (3.36). It is then easy to see, from (3.21), that δM_D is primarily a rank-two matrix contributing mass in the $q_2 - q_3$ subspace, thus ensuring the desired hierarchy. Although in this case one has to put in a hierarchy by hand the overall quark Yukawa coupling hierarchy need not exceed an order of magnitude, compared with 10^4 for the standard model.

2. *One-loop squark-gaugino graphs*

For this class of graphs the dominant mass contributions are due to gluino exchange $\delta M_{\tilde{g}}^q$ with smaller contributions ($\sim \alpha_W/\alpha_s$) due to the other gauginos. Again, in order to obtain the exact expression one must sum over all squark mass eigenstates propagating in the loop. For an order-of-magnitude estimate it suffices to consider the graph of Fig. 4, analogous to Fig. 2. The Yukawa matrices $H^{L,R}$ are replaced by the generation diagonal matrix $g_{\rm QCD} I_{3\times 3}$. Also notice that, because the gauginos are neutral, it is the down squarks (up squarks) which propagate in the graphs contributing to $\delta M_{\tilde{g}}^{d,(u)}$ which is opposite to what occurs in Fig. 2. One therefore expects $\delta M_{\tilde{g}}^d \gg \delta M_{\tilde{g}}^u$, given $\langle \nu_E \rangle \gg \langle N_E \rangle$ (or $\delta M_D^d \ll \delta M_D^u$). It is of course desirable to exploit this feature to help explain the first-generation anomaly $m_d > m_u$.

The mass contribution of Fig. 4 is given by

$$\delta M_{\tilde{g}}^q = \sum_{j,k} [|\tilde{k}_L\rangle \langle \tilde{k}_L | \tilde{h}_L \rangle \langle \tilde{h}_R | \tilde{j}_R \rangle \langle \tilde{j}_R | a_{\tilde{g}}^q (m_{jR}^2, m_{kL}^2)]_{\tilde{q}} , \tag{3.37}$$

where

$$a_{\tilde{g}}^d (m_{jR}^2, m_{kL}^2) \sim \frac{\alpha_s}{4\pi} \left[\frac{\mu_L^2 \mu_R^2 \mu'^2}{m^5} \right]_d \lesssim 8 \text{ GeV} \tag{3.38}$$

and we have taken $m_{\tilde{g}}^2, m_{kL}^2, m_{jR}^2, m_L'^2, m_R'^2 \sim m^2$. In obtaining the upper bound we have taken $\alpha_s \sim 0.1$ and made use of the same arguments leading up to (3.28). As for Fig. 2 we expect estimates obtained from (3.37) and (3.38) to be too large but within a factor of 2–3 of the exact contribution of this class of graphs, as well as suppression of order a_R^d / a_L for non-left-right-symmetric models. Again assuming near degeneracy of $M_{L,R}^2$, (3.37) can be rewritten, in analogy with (3.31), in the form

$$\delta M_{\tilde{g}}^q = a_{\tilde{g}}^q | \tilde{h}_L'' \rangle \langle \tilde{h}_R'' | + \delta_3 M_{\tilde{g}}^q . \tag{3.39}$$

$\delta_3 M_{\tilde{g}}$ is a rank-three matrix, suppressed by a factor $(\delta m_j^2 / m^2)^2$ relative to the rank-one term, and $|\tilde{h}_{L,(R)}'' \rangle = |\tilde{h}_{L,(R)} \rangle + O(\delta m_j^2 / m^2)$, in analogy with (3.32) and (3.33). From (2.7) and (3.19) it is clear that $|\tilde{h}_{L,(R)} \rangle$ is essentially equal to $|h_{L,R} \rangle$ [this would be true in supergravity theories even if the second term in expression (3.19) for $|\tilde{h} \rangle$ did not dominate since initially, in this context, $A_i \propto h_i$ with deviation at low energy due to renormalization] so that $(1 - \langle \tilde{h}'' | h \rangle_{L,R}^2)^{1/2} \sim \delta m_j^2 / m^2$. Therefore the rank-one term in (3.39) contributes mass primarily to third-generation quarks. This can certainly be of significance for the b quark, see (3.38). Hence our claim (cf. Sec. III A) that radiative corrections can appreciably increase (or decrease, depending on their sign) upper bounds on m_t obtained from ρ parameters constraints. The contribution of $\delta M_{\tilde{g}}$ to first- and second-generation quarks is greatly suppressed, but can certainly be at the level of 10–20 MeV for the down quarks, with $m_d > m_u$ a plausible consequence.

As for the isosinglet quark graph, if $M_{L,R}^2$ are not degenerate, Fig. 4 will preserve a mass hierarchy between first- and second-generation masses if one generation is decoupled by an order of magnitude in $H^{L,R}, h_{L,R}$. For a reasonable range of parameters, the contributions of Fig. 4 to s and d quarks will be of order m_s (perhaps larger, but excess can be offset by δM_D^d) and m_d, respectively.

To summarize, the dominance of the internal down-squark line over the up-squark line in one-loop graphs can explain both $m_c \gg m_s$ and $m_d > m_u$. The origin of this dominance, $M_d' \gg M_u'$, accounts for $m_t \gg m_b$ at the tree level as well.

3. *Other contributions to* δM^q

Among these are one-loop graphs with quarks and $\tilde{D}, \tilde{D}^c$ squarks in the loop, as in Fig. 5, leading to a mass contribution of the form

$$a_{\tilde{D}}^q H^L | h_L \rangle^* \langle h_R |^* H^R . \tag{3.40}$$

$a_{\tilde{D}}^u$ is given approximately by

$$a_{\tilde{D}}^u \sim \frac{1}{16\pi^2} \frac{a_L a_R M_d' A_4 \mu_D}{m_{\tilde{D}}^4} \ln \left[\frac{m_{\tilde{D}}^2}{M_d'^2} \right] \lesssim 10^{-3} \text{ GeV} , \tag{3.41}$$

where, in obtaining the upper bound we have taken $a_L a_R \sim 3 \times 10^3$ GeV, $M_d' \sim 500$ GeV (see Table III), $A_4 \mu_D \lesssim m_{\tilde{D}}^2$ (from color conservation), and $m_{\tilde{D}} \sim 5$–10 TeV (from K-$\bar{K}$ mixing, cf. Sec. III B 1). The contribu-

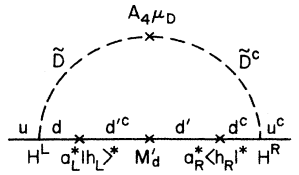

FIG. 5. Quark–isosinglet-squark graph.

tions of these graphs are, therefore, not important. Clearly, supersymmetry plays a crucial role since, without it, these graphs would provide the dominant radiative contribution to light-quark masses. Other one-loop graphs with gauge bosons and quarks in the loop only provide mass to third-generation quarks since the vertices are generation diagonal leading to contributions of the form $\delta m|h_L\rangle\langle h_R|$. Similarly, one-loop graphs containing ρ (or $\tilde{\rho}$) and mirror squarks (or mirror quarks) in the loop will also contribute mass only to third-generation quarks. As the gluino graphs these contributions should be taken into account when determining upper bounds on m_t from ρ parameter constraints.

Two-loop mass contributions $\delta M^q_{(2)}$ exist [see Figs. 3(a) and 3(b)] which, as the one-loop gluino graphs, can help explain $m_d > m_u$. This is similar to the situation in Ref. 4. For example, comparing Fig. 3(a), whose mass contribution, not including a negligible rank-three part, is of the form

$$a^d_{(2)} H^L H^{L\dagger} |h_L\rangle\langle h_R| H^{R\dagger} H^R \ , \tag{3.42}$$

with Fig. 2, one naively expects $a^d_{(2)} \sim m_c/16\pi^2 \sim 10$ MeV, at the level of m_d. The contribution of Fig. 3(b) will be similar. Again, $\mu'^2_d \gg \mu'^2_u$ implies $\delta M^d_{(2)} \gg \delta M^u_{(2)}$, as described. Note that contributions of two-loop graphs obtained from Fig. 3 by replacing D-quark lines with gluinos, although roughly of same magnitude, will be negligible for the first generation, since their matrix structure will be the same as that of Fig. 2 [see (3.31)]. Two-loop graphs with quark mass insertions, as in Fig. 5 will, of course, be negligible.

IV. PERTURBATION THEORY DERIVATION OF QUARK MASSES AND EIGENSTATES

The relevant mass eigenvalue equations are given in (3.2). We summarize below the perturbation theory calculation for the masses and left-handed mass eigenstates $|\Psi_L\rangle$. The right-handed eigenstates can then be obtained from (3.4) or by making the appropriate substitutions in $|\Psi_L\rangle$ corresponding to interchange of M, $M^\dagger$, see (3.2). From (3.5) $MM^\dagger$ is given by

$$MM^\dagger = V^{(0)} + V^{(1)} + V^{(2)} \ , \tag{4.1}$$

where

$$\begin{aligned} V^{(0)} &= M^0 M^{0\dagger} \ , \\ V^{(1)} &= M^0 M^{1\dagger} + M^1 M^{0\dagger} \ , \\ V^{(2)} &= M^1 M^{1\dagger} \ . \end{aligned} \tag{4.2}$$

From (3.34) and (3.39) the perturbation $M^1 (= \delta M)$ can be written as

$$\delta M = \tilde{a}_D |\tilde{H}\tilde{h}'_L\rangle\langle \tilde{H}\tilde{h}'_R| + a_{\tilde{g}} |\tilde{h}''_L\rangle\langle \tilde{h}''_R| + \delta_3 M \ , \tag{4.3}$$

where $\delta_3 M$, expected to be at the level of first-generation masses, contains all contributions to δM not otherwise specified above, i.e., $\delta_3 M_{D,\tilde{g}}, \delta M_{(2)}, \ldots$. The expansions for the eigenvalues and eigenvectors of $MM^\dagger$ are written as

$$\begin{aligned} m_i^2 &= m_i^{2(0)} + m_i^{2(1)} + m_i^{2(2)} + \cdots \ , \\ |\psi_{i_L}\rangle &= |\psi_{i_L}\rangle_{(0)} + |\psi_{i_L}\rangle_{(1)} + |\psi_{i_L}\rangle_{(2)} + \cdots \ . \end{aligned} \tag{4.4}$$

One makes the following identification of eigenstates with physical up quarks: $|\psi_{1_L}\rangle = |u_L\rangle$, $|\psi_{2_L}\rangle = |c_L\rangle$, $|\psi_{3_L}\rangle = |t_{3_L}\rangle$, $|\psi_{4_L}\rangle = |t_{4_L}\rangle$, with obvious generalization to the down-quark sector. Plugging these expressions into (3.2) yields the following perturbation equations which must be solved to obtain masses and eigenstates:

$$\sum_{j=0}^{n} (V^{(j)} - m^{2(j)}) |i\rangle_{n-j} = 0, \quad n = 0, 1, \ldots \ , \tag{4.5}$$

where $V^{(j)} = 0$, $j > 2$.

In carrying out the perturbative calculation one has to choose a suitable unperturbed orthonormal basis. Two of its elements are just the nonzero mass eigenstates of $V^{(0)}$ given in (3.8), i.e., $|3_{L,R}\rangle, |4_{L,R}\rangle$ with masses m_3^2, m_4^2, respectively. A convenient choice for the remaining basis vectors $|1_{L,R}\rangle, |2_{L,R}\rangle$, spanning the LH and RH tree-level massless subspaces, dictated by the form of δM_D (the dominant contribution to δM), (3.31), is

$$\begin{aligned} |2_{L,(R)}\rangle &= \begin{bmatrix} P_{L,(R)} |\tilde{H}\tilde{h}'_{L,(R)}\rangle \\ 0 \end{bmatrix} , \\ |1_{L,(R)}\rangle &= \begin{bmatrix} |1_{L,(R)}\rangle \\ 0 \end{bmatrix} , \end{aligned} \tag{4.6}$$

where $|1_{L,R}\rangle$ are uniquely determined by orthonormality. P_L, P_R are projection operators, defined by $P_L|h_L\rangle = P_R|h_R\rangle = 0$.

The perturbation calculation as outlined above is tedious and we only quote results here. The reader is referred to Ref. 4 for details of a similar calculation. However, it is not difficult to see from the form of (4.3), and Table III that in the combined basis (3.8) and (4.6), one is basically diagonalizing a matrix M of the form

$$M^{u,(d)} \sim \begin{array}{c} \\ \langle 1_L| \\ \langle 2_L| \\ \langle 3_L| \\ \langle 4_L| \end{array} \begin{array}{c} \begin{array}{cccc} |1_R\rangle & |2_R\rangle & |3_R\rangle & |4_R\rangle \end{array} \\ \begin{bmatrix} m_1 & m_1 & m_1 & (<)m_1 \\ m_1 & m_2 & m_2 & (<)m_2 \\ m_1 & m_2 & m_3 & (<)m_2 \\ (<)m_1 & (<)m_2 & (<)m_2 & m_4 \end{bmatrix} \end{array} , \tag{4.7}$$

where m_i is an entry at the level of ith generation masses and the inequalities are for δM^d. The masses of the first and second families are found via degenerate perturbation theory, solving the secular equation corresponding to the matrix

$$\Delta_{ij} = m_{i1} m_{j1}^* + m_{i2} m_{j2}^*, \quad i,j = 1,2, \tag{4.8}$$

where

$$m_{jk} = \langle j_L | M^1 | k_R \rangle, \quad j,k = 1,2,3,4 \ . \tag{4.9}$$

In the limit

$$|m_{22}| \gg |m_{11}|, \quad |m_{22}|^2 \gg |m_{12}|^2, |m_{21}|^2 , \tag{4.10}$$

the masses of the light families are given, to leading order, by

$$\begin{aligned} &m_{s,c}^2 \sim m_2^{2(2)} \sim |m_{22}|^2 , \\ &m_{d,u}^2 \sim m_1^{2(2)} \sim |m_{11}m_{22} - m_{12}m_{21}|^2/|m_{22}|^2 . \end{aligned} \tag{4.11}$$

The m_{ij} are given by

$$\begin{aligned} m_{22} &= \langle 2_L | (\tilde{a}_D | \tilde{H}\tilde{h}'_L \rangle \langle \tilde{H}\tilde{h}'_R | \\ &\quad + \tilde{a}_{\tilde{g}} | \tilde{h}''_L \rangle \langle \tilde{h}''_L | + \delta_3 M) | 2_R \rangle , \\ m_{12} &= \langle 1_L | (a_{\tilde{g}} | \tilde{h}''_L \rangle \langle \tilde{h}''_R | + \delta_3 M) | 2_R \rangle , \\ m_{11} &= \langle 1_L | (a_{\tilde{g}} | \tilde{h}''_L \rangle \langle \tilde{h}''_R | + \delta_3 M) | 1_R \rangle . \end{aligned} \tag{4.12}$$

The contribution of $a_{\tilde{g}}$ in (4.12) is expected to be at first-generation levels, since $|\tilde{h}_{L,R}\rangle \sim |h_{L,R}\rangle$ (cf. Sec. III B 2), thus ensuring validity of (4.10).

Radiative contributions to heavy-quark masses, of possible significance for m_b, are given by

$$m_k^{2(1)} = \langle k_L | V^{(1)} | k_L \rangle = m_{kk} m_k + m_{kk}^* m_k^* , \quad k = 3,4 . \tag{4.13}$$

Since $[c_{3_{L,R}}/(N_3^{L,R})^{1/2}]_d \sim 1$, one finds

$$|m_b^{\rm rad}| \sim |\langle h_L | M^1 | h_R \rangle_d| . \tag{4.14}$$

From (3.38) this can be as large as a few GeV.

The left-handed eigenstates, written in terms of the unperturbed basis vectors, $|j_L\rangle$, are given by

$$|\psi_{j_L}\rangle^q = \sum_{k=1,\ldots,4} x_{jk}^{Lq} |k_L\rangle . \tag{4.15}$$

To determine the KM, and NC mixing matrices it is convenient to isolate their isosinglet components, so we rewrite (4.15) in terms of a new basis where these appear explicitly. $|3_L\rangle$ and $|4_L\rangle$ are replaced by

$$\begin{aligned} |3'_L\rangle &= \begin{bmatrix} |h_L\rangle \\ 0 \end{bmatrix} \\ &= \frac{-1}{(N_{L_3}+N_{L_4})^{1/2}} [(N_{L_3})^{1/2} |3_L\rangle - (N_{L_4})^{1/2} |4_L\rangle] , \end{aligned} \tag{4.16}$$

$$\begin{aligned} |4'_L\rangle &= \begin{bmatrix} 0 \\ 0 \\ 0 \\ 1 \end{bmatrix} \\ &= \frac{1}{(N_{L_3}+N_{L_4})^{1/2}} [(N_{L_4})^{1/2} |3_L\rangle + (N_{L_3})^{1/2} |4_L\rangle) , \end{aligned}$$

where the expressions on the extreme RH side (RHS) are for $a_L, M' > 0$. The other basis elements remain the same. In terms of leading-order contributions to each of the x_{Ljk} one obtains

$$\begin{aligned} \sqrt{N_1}|\psi_1\rangle &= |1\rangle + x_{0,12}|2\rangle + \left[\frac{-x_{1,13}\sqrt{N_3}+x_{1,14}\sqrt{N_4}}{\sqrt{N_3}+\sqrt{N_4}}\right]|3'\rangle + \left[\frac{x_{1,13}\sqrt{N_4}+x_{1,14}\sqrt{N_3}}{\sqrt{N_3}+\sqrt{N_4}}\right]|4'\rangle , \\ \sqrt{N_2}|\psi_2\rangle &= x_{0,21}|1\rangle + |2\rangle + \left[\frac{-x_{1,23}\sqrt{N_3}+x_{1,24}\sqrt{N_4}}{\sqrt{N_3}+\sqrt{N_4}}\right]|3'\rangle + \left[\frac{x_{1,23}\sqrt{N_4}+x_{1,24}\sqrt{N_3}}{\sqrt{N_3}+\sqrt{N_4}}\right]|4'\rangle , \\ \sqrt{N_3}|\psi_3\rangle &= x_{1,31}|1\rangle + x_{1,32}|2\rangle + \left[\frac{-\sqrt{N_3}+x_{1,34}\sqrt{N_4}}{\sqrt{N_3}+\sqrt{N_4}}\right]|3'\rangle + \left[\frac{\sqrt{N_4}+x_{1,34}\sqrt{N_3}}{\sqrt{N_3}+\sqrt{N_4}}\right]|4'\rangle , \\ \sqrt{N_4}|\psi_4\rangle &= x_{1,41}|1\rangle + x_{1,42}|2\rangle + \left[\frac{\sqrt{N_4}-x_{1,43}\sqrt{N_3}}{\sqrt{N_3}+\sqrt{N_4}}\right]|3'\rangle + \left[\frac{x_{1,43}\sqrt{N_4}+\sqrt{N_3}}{\sqrt{N_3}+\sqrt{N_4}}\right]|4'\rangle , \end{aligned} \tag{4.17}$$

where $x_{i,jk} = \langle k | (|\psi_j\rangle_{(i)})$, i indicates the order in perturbation theory [see (4.4)], and the L subscripts are dropped. The $x_{i,jk}$ are given by

$$\begin{aligned} &x_{0,21} \sim \frac{m_{12}}{m_{22}} (x_{0,21}^u \sim 10^{-2}, \quad x_{0,21}^d \sim 10^{-1}), \quad x_{1,2k} \sim \frac{-m_{2k}^*}{m_k} \begin{bmatrix} x_{1,23}^u \sim x_{1,24}^u \sim 2\times 10^{-2} \\ x_{1,23}^d \sim 5\times 10^{-2}, \quad x_{1,24}^d \lesssim 10^{-4} \end{bmatrix} , \\ &x_{1,1k} \sim \frac{-m_{1k}^*}{m_k} + \frac{m_{2k}^*}{m_k}\frac{m_{12}^*}{m_{22}} \sim x_{1,2k}x_{1,12} \begin{bmatrix} x_{1,13}^u \sim x_{1,14}^u \sim 10^{-3}-10^{-4} \\ x_{1,13}^d \sim 10^{-2}-10^{-3}, \quad x_{1,14}^d \lesssim 10^{-5} \end{bmatrix} , \\ &x_{1,34} \sim \frac{-m_4^* m_{34}^* - m_3 m_{43}}{m_4^2 - m_3^2} (x_{1,34}^u \sim 10^{-2}, \quad x_{1,34}^d \sim 10^{-4}) , \end{aligned} \tag{4.18}$$

where, in obtaining the first three relations, use is made of (4.10). The remaining $x_{i,jk}$ are found from the following relations, obtained by imposing orthonormality of the eigenstates at each order:

$$x_{0,12}\sim -x^*_{0,21},\quad x_{1,k2}\sim -x^*_{1,2k},\quad x_{1,43}\sim -x^*_{1,34},$$
$$x_{1,k1}+x_{1,k2}x^*_{0,12}+x^*_{1,1k}\sim 0\ . \tag{4.19}$$

The order-of-magnitude estimates in (4.18) are obtained via the following relations, which are natural consequences of (3.8), (4.3), and (4.6):

$$\frac{m_{12}}{m_{22}}\sim\frac{m_1}{m_2},\quad m_{2k}\sim\frac{m_2 c_k}{\sqrt{N_k}},\quad m_{1k}\sim\frac{m_{12}}{m_k}\frac{c_k}{\sqrt{N_k}}\ ,$$
$$m_{34}\sim m_2\frac{c_3}{\sqrt{N_3}}\frac{c_4}{\sqrt{N_4}}\ . \tag{4.20}$$

In general, the $x^R_{i,jk}$ are expected to be of same order, although significant differences (e.g., factors of 3) are possible for non-left-right-symmetric models.

In the nondegenerate squark limit, where the observed mass hierarchy between first- and second-generation quarks is obtained by decoupling one generation of quarks by an order of magnitude in the Yukawa sector (cf. Sec. III B 1), the perturbative calculation yields similar expressions for the masses and eigenstates.

V. THE RADIATIVE KM MATRIX

The results of the previous section are used to obtain the charged-current mixing angles. As the RH quark mass eigenstates have small admixture with isodoublet mirror quarks there will be a RH $(V+A)$ KM matrix in addition to the usual LH $(V-A)$ KM matrix. The LH and RH KM matrices are given by

$$V^L_{u_i d_j}=\langle u_{iL}|P^L_0|d_{jL}\rangle\ ,$$
$$V^R_{u_i d_j}=\langle u_{iR}|P^R_0|d_{jR}\rangle\ , \tag{5.1}$$

where P^L_0 and P^R_0, given by

$$P^L_0=I-|4'_L\rangle\langle 4'_L|\ ,\quad P^R_0=|4'_R\rangle\langle 4'_R|\ , \tag{5.2}$$

project onto the LH and RH isodoublet subspaces, respectively. In general, entries in V^R are $\sim 10^{-1}$ or smaller than the corresponding entries in V^L so we do not discuss them here. The LH KM matrix can be read off from (4.17) and a few entries are given below, to leading order:

$$V^L_{us}\sim x^d_{0,21}\langle 1^u|1^d\rangle+x^{u*}_{0,12}\langle 2^u|2^d\rangle+\langle 1^u|2^d\rangle\ ,$$
$$V^L_{cd}\sim x^d_{0,12}\langle 2^u|2^d\rangle+x^{u*}_{0,21}\langle 1^u|1^d\rangle+\langle 2^u|1^d\rangle\ ,$$
$$V^L_{cb}\sim x^d_{1,32}\langle 2^u|2^d\rangle+\frac{x^*_{1,23}(N^u_3N^d_3)^{1/2}-x^{u*}_{1,24}(N^u_4N^d_3)^{1/2}}{[(N^u_4+N^u_3)(N^d_4+N^d_3)]^{1/2}}\ ,$$
$$V^L_{ub}\sim x^d_{1,31}\langle 1^u|1^d\rangle+x^d_{1,32}\langle 1^u|2^d\rangle+x^d_{1,32}x^{u*}_{0,12}\langle 2^u|2^d\rangle+\frac{x^{u*}_{1,13}(N^u_3N^d_3)^{1/2}-x^{u*}_{1,14}(N^u_4N^d_3)^{1/2}}{[(N^u_4+N^u_3)(N^d_4+N^d_3)]^{1/2}}\ , \tag{5.3}$$
$$V^L_{t_3 b}\sim\frac{(N^u_3N^d_3)^{1/2}}{[(N^u_4+N^u_3)(N^d_4+N^d_3)]^{1/2}},\quad V^L_{t_4 b}\sim\frac{-(N^u_4N^d_3)^{1/2}}{[(N^u_4+N^u_3)(N^d_4+N^d_3)]^{1/2}}\ .$$

Note that the equality $|h^u_L\rangle=|h^d_L\rangle$ (or $|3'^u\rangle=|3'^d\rangle$), guaranteed by $SU(2)_L$ invariance, ensures absence of tree-level contributions to V_{cb} and V_{ub}. It is also clear from (3.30), (3.32), (4.6), and $SU(2)_L$ invariance that $\langle 1^u|2^d\rangle\lesssim 0.1$. Our numerical estimates for the $x^L_{i,jk}$ (2.18) then imply

$$|V^L_{us}|,|V^L_{cd}|\sim 10^{-1}\ ,$$
$$|V^L_{cb}|,|V^L_{t_{3,4}s}|\sim 10^{-1}-10^{-2}\ ,$$
$$|V^L_{ub}|,|V^L_{t_{3,4}d}|\sim 10^{-2}-10^{-3}\ , \tag{5.4}$$
$$|V^L_{t_3 b}|,|V^L_{t_4 b}|\sim 1\ ,$$

certainly in general agreement with experiment. $V_{t_3 b}\sim V_{t_4 b}$ can have rich consequences for top-quark searches, especially if the top and mirror top are narrowly separated in mass.

The LH (RH) KM matrix will not be unitary due to admixture of isosinglet quarks in LH (RH) mass eigenstates. In particular, from (5.1),

$$V^L V^{L\dagger}_{ij}=\langle u_i|P_0|u_j\rangle_L\ ,$$
$$V^{L\dagger}V^L_{ij}=\langle d_i|P_0|d_j\rangle_L\ . \tag{5.5}$$

These are just the left-handed up and down NC mixing matrices (not including the $Q^{\rm em}$-dependent part) discussed in the next section.

VI. THE NEUTRAL-CURRENT MIXING MATRIX

The neutral-current mixing matrix (neglecting possible Z_L-Z_R mixing for $G_{LR,1R}$), is given by

$$V^{\rm NC}=\frac{e}{\sin\theta_W\cos\theta_W}[-\sin^2\theta_W Q^{\rm em}(I_L+I_R)$$
$$+\tau_3 P^L_0+\tau_3 P^R_0]\ , \tag{6.1}$$

where P_0^L, P_0^R, defined in (5.2) project onto the LH,RH isodoublet subspaces, respectively. The flavor-changing Z_L couplings for the quark mass eigenstates (in units of $e/2\sin\theta_w\cos\theta_w$) are

$$\begin{aligned} Z\psi_{iL}\psi_{jL} &= \langle \psi_{iL}|P_0^L|\psi_{jL}\rangle \\ &= -\langle \psi_{iL}|4'_L\rangle\langle 4'_L|\psi_{jL}\rangle \ , \\ Z\psi_{iR}\psi_{jR} &= \langle \psi_{iR}|P_0^R|\psi_{jR}\rangle \\ &= \langle \psi_{iR}|4'_R\rangle\langle 4'_R|\psi_{jR}\rangle \ . \end{aligned} \tag{6.2}$$

A few of these couplings are exhibited below, to leading order in the perturbation,

$$\begin{aligned} Z\psi_{2L}\psi_{3L} &\sim \frac{-x^{L*}_{1,23}N_{L_4}-x^{L*}_{1,24}(N_{L_3}N_{L_4})^{1/2}}{N_{L_3}+N_{L_4}} \ , \\ Z\psi_{1L}\psi_{3L} &\sim \frac{-x^{L*}_{1,13}N_{L_4}-x^{L*}_{1,14}(N_{L_3}N_{L_4})^{1/2}}{N_{L_3}+N_{L_4}} \ , \\ Z\psi_{1L}\psi_{2L} &\sim -[x^L_{1,23}(N_{L_4})^{1/2}+x^L_{1,24}(N_{L_3})^{1/2}] \\ &\quad \times[x^{L*}_{1,13}(N_{L_4})^{1/2} \\ &\quad +x^{L*}_{1,14}(N_{L_3})^{1/2}]/(N_{L_4}+N_{L_3}) \ . \end{aligned} \tag{6.3}$$

One notices immediately that $Z\psi_1\psi_2$, phenomenologically the most constrained coupling, is naturally the smallest, being the only one which arises at the two-loop order in the perturbation.

Some phenomenological consequences of the above couplings are discussed, in turn, below, beginning with the up-quark sector, where the effects are most dramatic. The quantity $N_4/(N_3+N_4)$, appearing often in (6.3), indicates the extent of seesaw suppression or lack thereof and is ~ 0.5 for both the LH and RH up quarks in the left-right-symmetric case [see Table III(a), example 1 and (3.8) and (3.10)]. The following numerical estimates are then obtained from (6.3), where use is made of (4.18):

$$\begin{aligned} &(zct_3)_{L,R}\sim(zct_4)_{L,R}\sim x^{L,R}_{1,23}\sim 10^{-2} \ , \\ &(zuc)_{L,R}\sim(x_{1,23}x_{1,13})_{L,R}\sim 10^{-5}-10^{-6} \ , \\ &(zut_3)_{L,R}\sim(zut_4)_{L,R}\sim(x_{1,13})_{L,R}\sim 10^{-3}-10^{-4} \ . \end{aligned} \tag{6.4}$$

Estimates for the couplings of the non-left-right-symmetric examples of Table III(a) (see examples 2 and 3) are of the same order. The $Zct_{3,4}$ couplings imply very large branching ratios for $Z\to t_{3,4}\bar{c}+\bar{t}_{3,4}c$, of order $10^{-4}-10^{-5}$. This estimate is obtained via the following approximation,[19] sufficiently reliable for our purposes for $m_t\sim 30$–70 GeV:

$$\begin{aligned} B(z\to t_{3,4}\bar{c}+t_{3,4}c) &\sim 2B(z\to t_{3,4}\bar{c}) \\ &\sim \frac{2[(zt_{3,4}c)^2_L+(zt_{3,4}\bar{c})^2_R]}{N_f} \ . \end{aligned} \tag{6.5}$$

N_f is the number of final-quark states accessible to diagonal Z decay. These decays should certainly be observed if LEP produces 10^7 Z's. Similarly, the $(Zut)_{L,R}$ estimates (6.4) imply $B(Z\to t_{3,4}\bar{u}+\bar{t}_{3,4}u)\sim 10^{-7}$. Finally, the $(Zuc)_{L,R}$ estimates imply D-$\bar{D}$ mixing, via tree-level Z exchange, at the level $\Delta M_D/M_D\sim 10^{-14}-10^{-15}$, which could be an order of magnitude or more above standard-model expectations.[20] Current upper limits are at or slightly below the 10^{-13} level.[21]

We now turn our attention to the down-quark sector, where flavor-changing effects vary significantly for the left-right and non-left-right-symmetric examples of Table III(b) due to large variation in $(N_4/N_3+N_4)_L$ (~ 0.1, 0.1, 0.07 for examples 1, 2, and 3, respectively). Estimates for flavor-changing Z couplings are given below:

$$\begin{aligned} &(z\,db)_{L,R}\sim 10^{-4} \ \text{(example 1)} \ , \\ &(z\,db)_L\sim 10^{-3}, \ (z\,bd)_R<10^{-4} \ \text{(examples 2 and 3)} \ , \\ &(z\,ds)_{L,R}\sim 10^{-6} \ \text{(example 1)} \ , \\ &(z\,ds)_L\sim 10^{-5}, \ (z\,ds)_R<10^{-6} \ \text{(examples 2 and 3)} \ , \\ &(zsb)_{L,(R)}\sim(z\,db)_{L,(R)}/\theta_c \ . \end{aligned} \tag{6.6}$$

The down-quark sector of left-right-symmetric models is not experimentally interesting due to large seesaw suppression (see example 1). However, this is certainly not the case for examples 2 and 3 which are not left-right-symmetric (or for left-right-symmetric models possessing isosinglet quarks mixing with mirror down quarks[16]). For example, if $(Z\,db)_L\sim 10^{-3}$ then B_d-$\bar{B}_d$ mixing ($\Delta M_B/M_B\sim 10^{-13}$ from Ref. 10) can be attributed to tree-level Z exchange, for which

$$\frac{\Delta M_{B_d}}{M_{B_d}}\sim\frac{G_F}{2\sqrt{2}}(z\,db)^2_L\tfrac{8}{3}f^2_{B_d}B_{B_d} \ .$$

$(Zsb)_L\sim 5\times 10^{-3}$ implies $B(b\to s\mu^+\mu^-)$ [$=9(Zsb)^2_L$ (Ref. 22)]$\sim 2\times 10^{-4}$ [the current upper bound for $b\to(d$ or $s)\mu^+\mu^-$ is 1.2×10^{-3} (Ref. 23)]. Finally, $K_L\to\mu^+\mu^-$ implies an upper bound of 2×10^{-5} for $(Z\,ds)_{L,R}$, which can certainly be saturated in examples 2 and 3. At this bound one obtains, from tree-level Z exchange,

$$\begin{aligned} B\left[K^+\to\sum_{i=1,2,3}\pi^+\nu_i\bar{\nu}_i\right] &\sim \frac{B(K^+\to\pi^-e\nu_e)}{\theta_c^2}\frac{(z\,ds)^2}{2} \\ &\sim 6\times 10^{-10} \ , \end{aligned}$$

which is to be compared with the standard-model upper bound[24] of 1–1.5×10^{-10}, 3×10^{-10} for $m_t\sim 50$, 80 GeV, respectively.

We end this section with a brief discussion of forward-backward asymmetry (A_{FB}) for $e^+e^-\to t_{3,4}\bar{t}_{3,4}, b\bar{b}$. This asymmetry is proportional to $a_e a_f$, where

$$a_f=\sqrt{\rho}[(Zff)_L-(Zff)_R] \tag{6.7}$$

($a_f=1$ in the standard model) and f is the final-state fermion. The relevant couplings are given by

$$\begin{aligned} &Z\psi_{3L}\psi_{3L}\sim\frac{N_{L_3}}{N_{L_3}+N_{L_4}}, \quad Z\psi_{3R}\psi_{3R}\sim\frac{N_{R_4}}{N_{R_3}+N_{R_4}} \ , \\ &Z\psi_{4L}\psi_{4L}\sim\frac{N_{L_4}}{N_{L_3}+N_{L_4}}, \quad Z\psi_{4R}\psi_{4R}\sim\frac{N_{R_3}}{N_{R_3}+N_{R_4}} \ . \end{aligned} \tag{6.8}$$

The forward-backward asymmetries for mass eigenstates Ψ_3, Ψ_4 will always be equal in magnitude and opposite in sign. For down quarks in examples 2 and 3 $(N_3/N_3+N_4)_L \sim 0.90$, 0.93, $(N_4/N_3+N_4)_R < 0.01$ implying 10% and 7% less forward-backward asymmetry, respectively, for $e^+e^- \to b\bar{b}$ than in the standard model. This deviation might be observable at LEP. Clearly, for the top system forward-backward asymmetry would be considerably smaller in magnitude, e.g., 30–100% than expected for the standard model.

VII. REMARKS ON NONPERTURBATIVE UNIFICATION

In the nonperturbative scenario of Maiani, Parisi, and Petronzio (MPP) (Ref. 11), QCD as well as the other interactions are asymptotically divergent so that the low-energy gauge couplings are not sensitive to their initial values at the ultraviolet cutoff scale Λ [$g_i(\Lambda) \gtrsim 1$ with equality among them not a necessity] but rather to the choice of field content, which controls their evolution, and the initial scale Λ. This would be the ideal scenario for the class of models we have been discussing since then *all initial couplings, Yukawa as well as gauge, could be* ~ 1, *with no special hierarchies required.*

Searches have been carried out[12] within the context of the supersymmetric standard model, to two-loop order, for solutions corresponding to $10^{14} \lesssim \Lambda \lesssim 10^{19}$. The field content singled out as yielding satisfactory predictions for α_s, $\alpha_{\rm em}$, and $\sin^2\theta_W$ is five ($n_g=5$) generations and less than four ($n_H<4$) Higgs doublets. As an illustration, for $\Lambda=M_P$, the $n_g=5$, $n_H=0$ solution of Cabibbo and Farrar[12] gives $\alpha_s \sim 0.08$, $\alpha_{\rm em}^{-1} \sim 137$, $\sin^2\theta_W \sim 0.222$ at Λ_F. Given that two-loop contributions to $\sin^2\theta_W$ are at the 15% level, higher-loop effects can be substantial and these numbers should be regarded as acceptable. It should also be pointed out that this result has been obtained neglecting two-loop Yukawa coupling effects as well as changes in evolution below $m_{\rm SUSY}$, i.e., the authors have taken $m_{\rm SUSY} \sim \Lambda_F$.

Above m_s the one-loop renormalization coefficients A_i, $i=1,2,3$ [at one loop $d\alpha_i/d\ln E=(A_i/2\pi)\alpha_i^2$] for $n_g=5$, $n_H=0$ are given by $A_3=1$, $A_2=4$, and $A_1=\frac{50}{3}$. Remarkably, for the standard-model gauge group, the field content of Tables I and II [without the charged components of the would-be $SU(2)_R$ Higgs doublets] together with four lepton families (three ordinary and one mirror) and one more set of isosinglet down quarks D, D^c (these may have several crucial roles to play), *yields the same one-loop renormalization coefficients* A_i *above* $m_{\rm SUSY}$. This is readily seen for A_3 and A_2 as the number of color triplets and $SU(2)_L$ doublets is the same in both cases (for A_1 use $A_1=\sum Q_{Yi}^2/4$). Certainly one has to do an explicit calculation taking two-loop effects (these will differ in our case), including Yukawa couplings, and the SUSY mass gap, $m_{\rm SUSY}$, into account, as in Maiani and Petronzio.[12] However the exact result should not differ from one-loop results (with SUSY mass gap neglected) by more than 10–20%. Nonperturbative unification is therefore extremely promising for this class of models, at least for G_{1Y}. For G_{1R}, G_{LR} low-energy predictions for α_s will almost certainly be acceptable since A_3 remains unaltered. However some modification in color-singlet, electroweak field content is probably required both to obtain successful predictions for $\alpha_{\rm em}, \sin^2\theta_W$ as well as to obtain a light neutrino seesaw, with the $SU(2)_R$- or $U(1)_R$-breaking scale becoming an important parameter in the evolution of electroweak gauge couplings. Nevertheless, the field content appears to be in the right ballpark.

Finally, we note that the additional isosinglet down quarks D, D^c required in order to obtain the desired value of A_3, may have several other functions. As remarked in Sec. III A (Ref. 16), a vectorlike down-quark mixing exclusively with mirror down quarks can allow for $m_t \sim 50$–100 GeV without having to break isospin explicitly in the superpotential, while simultaneously satisfying ρ parameter constraints. Also, in order to prevent rapid proton decay, a second vectorlike down quark coupling leptons (but not quarks) to squarks would be required if m_μ is to be generated via a graph analogous to Fig. 2. Presumably, the τ would acquire its mass via an ordinary-mirror lepton seesaw.

VIII. CONCLUSION

We review the main features of the models discussed, summarize some of their phenomenological implications, and end with a brief discussion of related issues some of which are currently under investigation. The models are supersymmetic, with soft SUSY breaking assumed. The left-right-symmetric gauge group as well as its subgroups have been considered. The quark content consists of three ordinary families, a fourth mirror family, and a pair of isosinglet down quarks D, D^c (see Table I). The third and mirror quark families obtain mass at the tree level while the light quarks remain massless (cf. Sec. III A). A $Z_3 \otimes Z_2$ symmetry (this choice is not unique) helps accomplish this by preventing ordinary quark–Higgs-doublet Yukawa couplings at the tree level (cf. Sec. II). The light quarks acquire their mass radiatively (cf. Sec. III B) primarily via graphs with squarks and isosinglet quarks (Figs. 2 and 3) as well as squarks and gluinos (Fig. 4) in the loops. Supersymmetry therefore plays a crucial role. The KM matrix is generated radiatively as well (cf. Sec. V).

The observed quark mass and KM mixing hierarchies are obtained without any special Yukawa coupling hierarchy among the different families (they can all be ~ 1) or horizontal symmetries if the ordinary 3×3 squark submatrices M_L^2, M_R^2 [see (3.18)] are degenerate at the 10% level or less. At the other extreme, if these matrices are not degenerate all Yukawa couplings involving one generation of quarks must be suppressed by an order of magnitude relative to the remaining couplings. The observed isodoublet mass splittings $m_t \gg m_b$, $m_c \gg m_s$, $m_d > m_u$ receive a unified understanding, with all of them attributed to the mirror quark mass inequality $M_d' \gg M_u'$. This inequality, associated with $SU(2)_L$ breaking, can be obtained without explicit isospin breaking in the superpotential with SUSY again playing a crucial role (cf. Sec. II B). Because of ordinary-mirror quark mixing radiative

flavor-changing Z couplings with important phenomenological implications emerge (cf. Sec. VI) satisfying $Zq_1q_2 \ll Zq_1q_3 \ll Zq_2q_3$. Because of SUSY if one adds a second set of light isosinglet down quarks to the superfield content these models provide a very promising setting for nonperturbative MPP unification (cf. Sec. VIII). Therefore the possibility exists that *all dimensionless couplings, gauge as well as Yukawa, could be* ~ 1 *at* M_P.

The radiative FCNC's characteristic of these models lead to interesting flavor-violating Z decays (cf. Sec. VI). For example, if $m_t < m_Z - m_c$ then the Zct coupling implies $B(Z \to \bar{c}t + c\bar{t}) \sim 10^{-4} - 10^{-5}$, with similar branching ratio for charm + mirror top (t') if $m_{t'} < m_Z - m_c$. These decays should be observable at LEP given 10^7 Z's. In the down-quark sector the $Z\,db$ coupling may be large enough to induce B_d-$\bar{B}_d$ mixing at observed levels via tree-level Z exchange. Because of ordinary-mirror quark mixing forward-backward asymmetries for $e^+e^- \to b\bar{b}$, $t\bar{t}$ may be as much as 10%, 30–100% smaller than standard-model expectations, respectively. From various box graphs contributing to ΔM_K (cf. Sec. III B 1) a safe scale for soft SUSY breaking is ~ 5–10 TeV.

The ρ parameter constraints on isodoublet mass splittings imply $\min(m_t, m_{t'}) \lesssim 40$ GeV in the left-right-symmetric case (cf. Sec. III A). For the non-left-right-symmetric models $\min(m_t, m_{t'}) \sim 50$–$100$ GeV is possible if isospin is explicitly broken in the superpotential. Similar mass for the lighter top is possible in the left-right-symmetric case, and more generally, in models without explicit isospin breaking in the superpotential, if there is an additional pair of isosinglet quarks mixing exclusively with mirror down quarks.[16] The mirror bottom quark is always considerably heavier than the top or mirror top quarks with typical mass $\lesssim 300$ GeV. Respective KM mixing angles of the top and mirror top are of the same order. In particular, $V_{tb} \sim V_{t'b}$ can have rich implications for top-quark searches, especially if the top and mirror top are narrowly separated in mass.

The combination of three ordinary families and one mirror family is uniquely singled out by the observed quark mass hierarchy. For example, if there were three ordinary families and more than one mirror family then, in general, ordinary-mirror quark mixing would induce a rank-two or -three tree-level contribution to ordinary quark masses spoiling the mass hierarchy. With four ordinary families and one mirror family the top-quark mass would have to be a radiative quantity which is unlikely. Finally, with four ordinary families and two mirror families although only two ordinary families would pick up mass at the tree level the largest radiative contributions would, in general, be of rank two spoiling the mass hierarchy between the first and second families.

Many issues associated with this class of models remain to be investigated. Currently work is in progress on extension of the mechanisms discussed to the leptonic sector. Presumably, the τ acquires the bulk of its mass via ordinary-mirror lepton mixing. The μ and e can acquire their masses radiatively via graphs analogous to Figs. 2–5. Isosinglet quarks propagating in these loops with Yukawa couplings to leptons and ordinary squarks will have to be different than those appearing in Figs. 2 and 3 in order to prevent proton decay. This is interesting because the presence of two sets of isosinglet down quarks is favored by MPP unification. Generation of charged lepton masses will, in turn, lead to neutrino Dirac masses which must be seesaw suppressed to obtain ultralight neutrinos.

A number of issues require detailed numerical investigation of renormalization-group evolution. For example, it is important to check whether, within the context of no-scale supergravity, the ordinary squark mass matrices at low energies can be degenerate at or below the 10% level despite the presence of large Yukawa couplings. It is also of interest to check explicitly whether, within the context of MPP unification, acceptable low-energy gauge couplings can be obtained, taking two-loop effects including Yukawa couplings into account. A study of CP violation including calculation of the neutron electric dipole moment in these models is also worthwhile. Finally, the field content and discrete symmetries required by this class of models can, in principle, be obtained from the superstring. Because initial Yukawa and, possibly, gauge couplings can be of the same order these models could remove a lot of the burden from the superstring and a search for two-generation string vacua is, therefore, strongly advocated.

Note added. After completion of this work it was brought to my attention that supersymmetric models with one mirror family have recently been considered in Ref. 25 as well, although there the quark mass and mixing hierarchies are put in by hand at the tree level. These authors have found similar branching ratios for $Z \to c\tilde{t} + \bar{c}t$. I would like to thank Jon Rosner for pointing this work out to me.

ACKNOWLEDGMENTS

I would like to thank my collaborators Rabi Mohapatra and B. S. Balakrishna for numerous helpful discussions throughout this work. I would also like to thank Jon Rosner for encouraging me to investigate flavor-changing neutral-current effects as well as for a critical reading of the original manuscript and his continued support. I have also had useful conversations with K. S. Babu, Partha Majumdar, and Jogesh Pati. This work was supported by a Grant from the National Science Foundation, submitted in partial fulfillment of requirements for the Ph.D. in Physics at the University of Chicago.

APPENDIX: δM_D FROM DIAGONALIZATION of $\tilde{M}^2$

In the limit where $M^2_{L,R}$ (3.18) are diagonal and degenerate and $\tilde{M}^2$ is invariant under P, the latter is easily diagonalized. It is then straightforward to obtain the exact expression for δM_D. Note that for models which are initially left-right-symmetric and invariant under P, which also satisfy $\delta m_j^2/m^2 \lesssim 0.1$ (3.30), the true squark mass matrix is only a small perturbation about this limit. The eigenvalue problem reduces to two simpler ones, each yielding four eigenstates, given by

$$\tilde{\psi}_L = \pm \tilde{\psi}_R, \quad (B \pm A)\tilde{\psi}_L = m^2 \tilde{\psi}_L \ , \tag{A1}$$

where the mass eigenstates are given by $\Psi = (\tilde{\Psi}_L, \tilde{\Psi}_R)$ and the basis for $\tilde{\Psi}_L$ and $\tilde{\Psi}_R$ is $(\tilde{q}_i, \tilde{q}\,')$ and $(\tilde{q}_i^{\,c*}, \tilde{q}^{\,'c*})$, respectively. The matrices A and B are given by

$$A = \begin{bmatrix} 0 & \mu^2 |\tilde{h}\rangle \\ \mu^2 \langle \tilde{h}| & \mu'^2 \end{bmatrix}, \quad B = \begin{bmatrix} m^2 I_{(3\times 3)} & 0 \\ 0 & m'^2 \end{bmatrix}, \tag{A2}$$

where the ρ^2 entries in (3.18) are omitted since they are negligible, cf. Sec. III B 1. Orthonormal solutions of (A1) are given by

$$\begin{aligned}
&m_1^{2\pm} = m^2 \ , \\
&m_3^{2\pm} = \tfrac{1}{2}\{(m'^2 \pm \mu'^2 + m^2) - [(m'^2 \pm \mu'^2 - m^2)^2 + 4\mu^4]^{1/2}\} \ , \\
&m_2^{2\pm} = m^2 \ , \\
&m_4^{2\pm} = \tfrac{1}{2}\{(m'^2 \pm \mu'^2 + m^2) - [(m'^2 \pm \mu'^2 - m^2)^2 + 4\mu^4)]^{1/2}\}, \\
&\psi_{iL}^{\pm} = \pm \psi_{iR}^{\pm} = \begin{bmatrix} |i\rangle \\ 0 \end{bmatrix}, \quad i = 1,2 \ , \\
&\psi_{kL}^{\pm} = \pm \psi_{kR}^{\pm} = \frac{1}{(\tilde{N}_k^{\pm})^{1/2}} \begin{bmatrix} \tilde{c}_k^{\pm} |\tilde{h}\rangle \\ 1 \end{bmatrix}, \\
&\tilde{c}_k^{\pm} = \frac{\pm (m_k^{2\pm} \mp \mu'^2 - m'^2)}{\mu^2}, \quad k = 3,4 \ .
\end{aligned} \tag{A3}$$

δM_D is, in turn, given by

$$\delta M_D^q = a_D^q H |h\rangle^* \langle h|^* H \ , \tag{A4}$$

where

$$a_D = \sum_{k=3,4;\pm} \pm \left[\frac{\tilde{c}_k^{\pm}}{(\tilde{N}_k^{\pm})^{1/2}} \right]^2 \frac{1}{16\pi^2} \frac{\mu_D}{\mu_D^2 - m_k^{\pm 2}} \times \left[m_k^{\pm 2} \ln \left[\frac{m_k^{\pm 2}}{\mu_D^2} \right] \right] \quad (F_c = 2) \ . \tag{A5}$$

In obtaining (A5) we have summed contributions of all graphs contributing to δM_D, each with a different squark mass eigenstate propagating in the loop. As a numerical example for δM_D^u, taking $m' = m = \mu_D = 5$ TeV, $\mu'^2 = 5$ TeV^2, $\mu = 4.5$ TeV, (A5) implies $a_D^u = 3.25$ GeV. The estimate (3.25) for Fig. 2 would yield $a_D^u = 8.3$ GeV which is large but differs by less than a factor of 3. This is generally the case for all numerical examples we have considered.

[1] J. Gasser and H. Leutwyler, Phys. Rep. **87**, 77 (1982).

[2] S. Weinberg, Phys. Rev. Lett. **29**, 388 (1972); H. Georgi and S. L. Glashow, Phys. Rev. D **6**, 2977 (1972); **7**, 2457 (1973); R. N. Mohapatra, *ibid.* **9**, 3461 (1974); S. M. Barr and A. Zee, *ibid.* **15**, 2652 (1977); **17**, 1854 (1978); S. M. Barr, *ibid.* **21**, 1424 (1980); R. Barbieri and D. V. Nanopoulos, Phys. Lett. **91B**, 369 (1980); **95B**, 43 (1980); R. Barbieri, D. V. Nanopoulos, and A. Masiero, *ibid.* **104B**, 194 (1981); R. Barbieri, D. V. Nanopoulos, and D. Wyler, *ibid.* **106B**, 303 (1981); S. M. Barr, Phys. Rev. D **24**, 1895 (1981); M. Bowick and P. Ramond, Phys. Lett. **103B**, 338 (1981); S. M. Barr, Phys. Rev. D **31**, 2979 (1985).

[3] B. S. Balakrishna, Phys. Rev. Lett. **60**, 1602 (1988).

[4] B. S. Balakrishna, A. L. Kagan, and R. N. Mohapatra, Phys. Lett. B **205**, 345 (1988).

[5] The particular choice of an isosinglet color-triplet scalar within the context of these models was suggested by R. N. Mohapatra.

[6] This was pointed out by R. N. Mohapatra.

[7] A. S. Joshipura, Phys. Rev. D **39**, 878 (1989).

[8] Models in which ordinary quarks acquire mass via mixing with mirrors have previously been considered by F. del Aguila and M. J. Bowick, Nucl. Phys. **B224**, 107 (1983); F. del Aguila, M. Dugan, B. Grinstein, L. Hall, G. G. Ross, and P. West, *ibid.* **B250**, 225 (1985); F. del Aguila, Ann. Phys. (N.Y.) **165**, 237 (1985); A. L. Kagan and C. H. Albright, Phys. Rev. D **38**, 917 (1988).

[9] M. Veltman, Nucl. Phys. **B123**, 89 (1977); J. J. van der Bij and F. Hoogeveen, *ibid.* **B283**, 477 (1987), and references therein; U. Amaldi *et al.*, Phys. Rev. D **36**, 1385 (1987).

[10] ARGUS Collaboration, H. Albrecht *et al.*, Phys. Lett. B **192**, 245 (1987).

[11] L. Maiani, G. Parisi, and R. Petronzio, Nucl. Phys. **B136**, 115 (1978).

[12] N. Cabibbo and G. R. Farrar, Phys. Lett. **125B**, 107 (1982); L. Maiani and R. Petronzio, Phys. Lett. B **176**, 120 (1986).

[13] The coupling of a singlet y to Higgs doublets and resulting implications for the Higgs potential have been considered by several authors within the context of the SUSY standard model. See H. P. Nilles, Phys. Rep. **110**, 1 (1984), and references therein.

[14] See Kagan and Albright (Ref. 8).

[15] R. Barbieri and L. Maiani, Nucl. Phys. **B224**, 32 (1983).

[16] A. L. Kagan (in preparation).

[17] For a detailed analysis of box graphs contributing to ΔM_K containing squarks and gluinos in the loops, see F. Gabbiani and A. Masiero, INFN-Sezione de Padova Report No. DFDP 88/TH/8, 1988 (unpublished) and M. Dugan *et al.*, Nucl. Phys. **B255**, 413, (1985). Box graphs contributing to ΔM_K containing isosinglet color-triplet scalars in the loop were pointed out to me by K. S. Babu.

[18] A. B. Lahanas and D. V. Nanopoulos, Phys. Rep. **145**, 1 (1987), and references therein.

[19] V. Ganapathi *et al.*, Phys. Rev. D **27**, 579 (1983).

[20] L. L. Chau, Phys. Rep. **95**, 1 (1983).

[21] E-691 Collaboration, J. C. Anjos *et al.*, Phys. Rev. Lett. **60**, 239 (1988).

[22] G. Eilam and T. G. Rizzo, Phys. Lett. B **188**, 91 (1987).

[23] CLEO Collaboration, A. Bean *et al.*, Phys. Rev. D **35**, 3533 (1987).

[24] J. Ellis, S. S. Hagelin, and S. Rudaz, Phys. Lett. B **192**, 201 (1987).

[25] W. Buchmüller and M. Gronau, Phys. Lett. B **220**, 641 (1989).